

XI

Structural Stability

XI.1 Introduction

In the analysis of the behaviour of slender members performed until now, equilibrium and compatibility conditions have been used in order to find the internal forces and deformations. In the simplest cases, a structure's safety is evaluated by confirming that the maximum values computed for the stresses are lower than the allowable stress defined for the material the structure is made of. This is a necessary condition for structural safety, but it may not be sufficient, either because the deformations are limited for some reason, or because there is the risk that the equilibrium configuration of the structure is not stable, i.e., that *buckling* may occur. In this chapter the study of the conditions under which a structure is stable is introduced. Buckling may occur when there are compressive internal forces in the structure. In fact, while tensile forces may only do work if the material deforms or ruptures, for the case of compression there is a third possibility – buckling – which consists of a lateral deflection of the material, in relation to direction of actuation of the compressive forces. The main subject of this chapter is the investigation of the conditions under which buckling occurs in a slender member.

The concept of stability may be easily understood by means of the classical example of a sphere which is in static equilibrium on a horizontal surface, as represented in Fig. 154.

In this example physical evidence makes a deeper analysis unnecessary: in the first case (concavity) the equilibrium is stable, while in the second case (convexity) it is unstable. However, in the study of the stability of deformable bodies, the physical evidence is almost completely lost, since stability or instability are determined by how the internal forces and stiffnesses are distributed inside the body which, in most cases, is not an intuitive matter.

In order to solve this problem, two distinct approaches are usually taken into consideration. Both of them are easily understood by analogy with the example of the sphere.

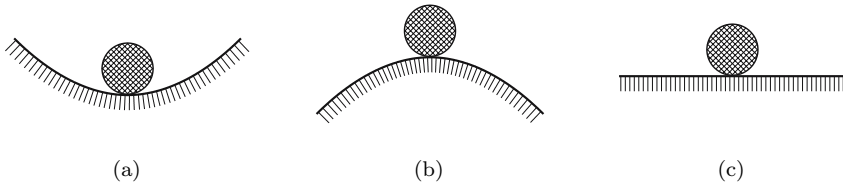


Fig. 154. Equilibrium of a sphere on a horizontal surface: (a) Stable equilibrium; (b) Unstable equilibrium; (c) Neutral equilibrium

– The first is based on the concept of potential energy. In the example of Fig. 154, the height of a point on the supporting surface defines the potential energy. The equilibrium position is an extremum of this energy. If this extremum is a minimum, the equilibrium will be stable (Fig. 154a), if it is a maximum, it will be unstable (Fig. 154b).

In the equilibrium configuration of a deformed body the potential energy also reaches an extremum (see Sect. XII.5). However, in this case it has two distinct components: the potential energy of the applied forces and the potential energy stored by the elastic deformation of the body. Both vary when the deformation field in the body varies. In the same way as in the example of the sphere, the stability or instability of an equilibrium configuration may be investigated by determining if it corresponds to a minimum or to a maximum of the potential energy.

– The second approach is based on the analysis of the effect of perturbations to the equilibrium configuration. If the perturbation is amplified, the equilibrium state is unstable; if it is damped, the equilibrium will be stable. In the example of the sphere the perturbation may be given by a small displacement from the equilibrium point. It is obvious that in the case of Fig. 154a, when the force causing the displacement disappears, the sphere returns to the equilibrium position, which means that the perturbation is damped, i.e., that the equilibrium is stable. In the case of Fig. 154b any displacement from the equilibrium point, no matter how small it is, will cause the sphere to roll away from the equilibrium configuration, which means that the perturbation is *amplified*. The situation of neutral equilibrium (Fig. 154-c) represents the transition from the stable to the unstable phase. It corresponds to a situation in which the deformation state of the structure can be changed without disturbing the equilibrium between internal and external forces. This is the so-called *critical phase*.

In the analysis contained in this chapter the second approach will be used, since it allows a better physical understanding of the buckling phenomenon. Furthermore, with this option, the difficulties arising when the energy method is applied in cases where energy dissipation takes place (plastic and viscous deformation), may be circumvented.

The analysis of the effect of perturbations requires the analysis of the equilibrium in a deformed configuration of the structure, as opposite to the

analysis of the effects of the internal forces in slender members described in the preceding chapters, where the equilibrium conditions have always been stated in the undeformed configuration. For these reasons, the theories relating to the buckling phenomena are sometimes called *second-order theories*, in which the interaction between the deformations and the internal forces is taken into consideration. It is this interaction (influence of the deformation on the internal forces and vice versa) that may cause instability.

The need to take this interaction into account means that the structural behaviour may not be accepted as geometrically linear, since we cannot consider that the geometry of the structure remains unchanged. As a consequence, the superposition principle cannot generally be used when buckling is analysed.

Since buckling is always associated with compressive stresses, we consider in this Chapter that compressive axial forces and stresses are positive.

XI.2 Fundamental Concepts

Before the main subject of this chapter – the buckling of axially compressed slender members – is tackled, some very simple examples are analysed in detail, in order to introduce fundamental concepts related to the study of structural stability.

XI.2.a Computation of Critical Loads

In accordance with the considerations above, the stability of a structure may be analysed by computing its *critical load*, i.e., the load corresponding to the situation in which a perturbation of the deformation state does not disturb the equilibrium between the external and internal forces. In order to illustrate these considerations, we first analyse the column represented in Fig. 155a.

It is obvious that this structure is stable in the case of a tensile axial force and unstable under compression. In order to give the structure the capacity to withstand compressive forces, a spring with stiffness E is placed in point B , as represented in Fig. 155b. The critical load of this new structure may be found by analysing the force F which is needed to introduce the perturbation represented by the horizontal displacement δ . Considering this displacement as infinitesimal and denoting by θ the rotation angle of the bars, we have $\sin \theta = \frac{\delta}{l} \approx \theta$ and $N \approx P$. From the horizontal equilibrium condition of the forces acting in node B we get ($E\delta$ is the force in the spring)

$$2N \sin \theta + F = E\delta \Rightarrow F = \left(E - \frac{2P}{l} \right) \delta .$$

If force F is positive, i.e., if it takes the same direction as the displacement δ , the structure is stable, since it is necessary to apply a force to disturb the equilibrium configuration. A negative value of force F , however, means that it

is necessary to apply a force in order to prevent displacement δ from increasing, i.e., that the perturbation is amplified. Thus, the structure is unstable. The critical load corresponds to the transition situation ($F = 0$), where the equilibrium is neutral, since the perturbation δ does not affect the equilibrium. The critical load is then

$$F = 0 \Rightarrow P = P_{cr} = \frac{El}{2}.$$

The quantity $\frac{F}{\delta} = E - \frac{2P}{l}$ represents the horizontal stiffness of the structure in point B . When it becomes negative, the structure becomes unstable.

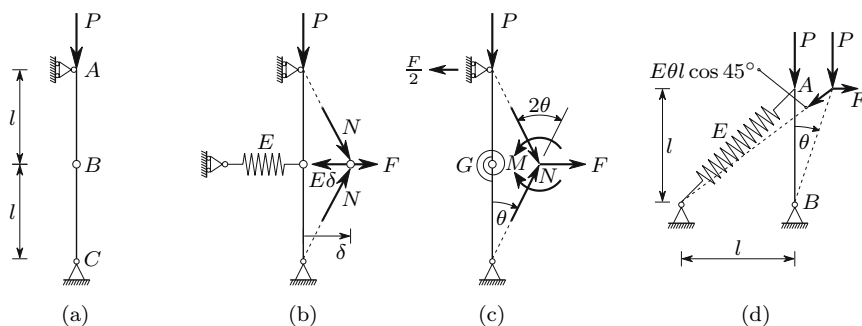


Fig. 155. Simple examples of computation of the critical load

In the structure represented in Fig. 155c, the stability under compressive loading is increased by means of a rotation spring linking the extremities of the two bars converging in point B . The spring has a stiffness G , which means that it is necessary to apply a bending moment $M = 2G\theta$ to introduce the relative rotation 2θ between bars \overline{AB} and \overline{BC} . The relation between the load P , the force F and the rotation θ may be found by expressing the bending moment in the rotation spring as a function of the load P . The reaction force in support A is $\frac{F}{2}$, as is easily concluded by means of the balance condition of the moment with respect to point C . Considering the rotation angle θ as infinitesimal, we get

$$\begin{cases} \sin \theta \approx \theta \\ \cos \theta \approx 1 \end{cases} \Rightarrow P \times \theta l + \frac{F}{2} \times l = 2G\theta \Rightarrow F = \left(\frac{4G}{l} - 2P \right) \theta.$$

In the critical situation the perturbation θ does not disturb the equilibrium, which means that the critical load is that corresponding to $F = 0$, i.e.,

$$F = 0 \Rightarrow P = P_{cr} = \frac{2G}{l}.$$

From a qualitative point of view, this problem is analogous to the compression of a pin-ended bar. In fact, even without a deeper analysis, we intuitively

know that the shorter the bar and the higher its bending stiffness (here represented by G), the higher the load required to induce buckling in a compressed bar.

The critical load of the structure represented in Fig. 155d may be computed in the same way, by considering the infinitesimal perturbation θ caused by the force F . The rotation θ induces an elongation $\theta l \cos 45^\circ$ in the spring. The balance condition of the moment with respect to node B of the forces acting in node A yields

$$F \times l + P \times \theta l + \overbrace{E\theta l \frac{\sqrt{2}}{2}}^{\text{force in the spring}} (\sin 45^\circ \theta l - \cos 45^\circ l) = 0 .$$

As in the two other examples, the critical load corresponds to $F = 0$, which leads to (θ may be disregarded in the subtraction $1 - \theta$)

$$F = 0 \Rightarrow P\theta l = E\theta l \frac{\sqrt{2}}{2} (l - \theta l) \frac{\sqrt{2}}{2} \Rightarrow P = \frac{El}{2} .$$

XI.2.b Post-Critical Behaviour

The three structures analysed in Subsect. XI.2.a exhibit different behaviour after the critical load is reached. In order to analyse the differences it is necessary, not only to consider deformed configurations, but also to abandon the infinitesimal deformation domain and consider arbitrary values for the parameters defining the deformation.

Taking the first of the above analysed structures (Figs. 155a and 156a), now with the deformation defined by angle θ (Fig. 156b), the load P necessary to balance the force acting in the spring for a given value of θ , may be computed by means of the horizontal balance condition of the forces acting in node B . Thus, we have (F_s is the force in the spring)

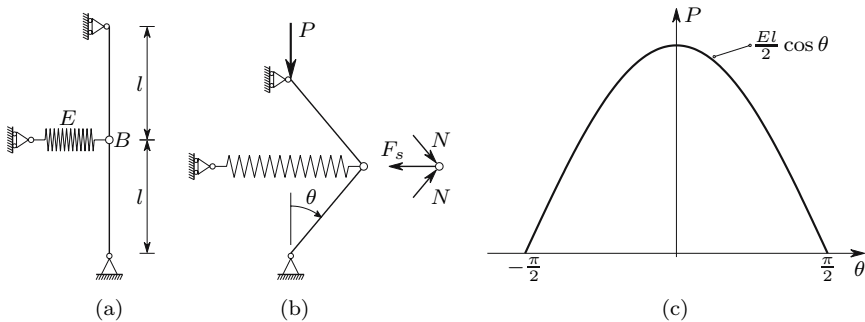


Fig. 156. Unstable post-critical behaviour

$$\begin{cases} N = \frac{P}{\cos \theta} \\ F_s = El \sin \theta \end{cases} \Rightarrow 2N \sin \theta = F_s \Rightarrow 2P \frac{\sin \theta}{\cos \theta} = El \sin \theta .$$

In the undeformed configuration ($\theta = 0$) equilibrium occurs for any value of the load P , since $\sin \theta = 0$. However, when there is deformation ($\theta \neq 0$), the equilibrium condition requires that P takes the value

$$P = \frac{El}{2} \cos \theta .$$

From this expression we conclude that, in a deformed configuration, equilibrium is only possible for values of P that are lower than the critical load $\frac{El}{2}$. Furthermore, we conclude from the relation between P and θ (Fig. 156c) that, in a deformed configuration, the stiffness is negative, since an increase in the deformation θ corresponds to a decrease of the load P . As seen in Subsect. XI.2.a, this means that the deformed situation is unstable. This structure is said to have an *unstable post-critical behaviour*. The critical load obtained for the undeformed configuration is, therefore, the maximum load that can be supported by the structure.

Let us now consider the second of the structures analysed in Subsect. XI.2.a (Figs. 155c and 157a).

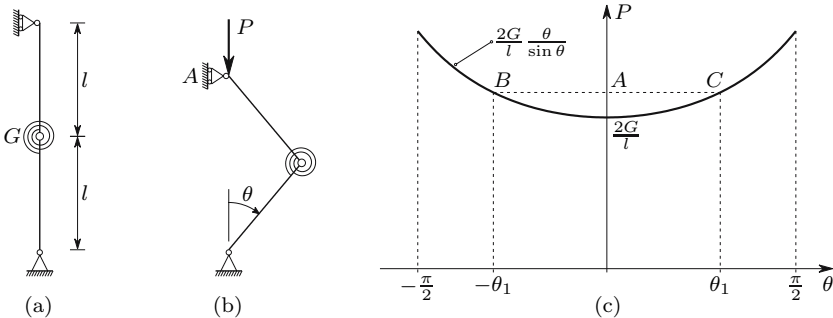


Fig. 157. Stable post-critical behaviour

The equilibrium condition in the deformed configuration defined by a given value of angle θ (Fig. 157b), may be established by computing the bending moment caused by load P in the rotation spring. Since the reaction force in support A vanishes, we have

$$Pl \sin \theta = 2G\theta \Rightarrow P = \frac{2G}{l} \frac{\theta}{\sin \theta} . \tag{248}$$

Since θ (measured in radians) is always superior to $\sin \theta$, the only possible equilibrium configuration for values of P that are inferior to $\frac{2G}{l}$ is the undeformed configuration ($\theta = 0$). Furthermore, the first of 248, confirms that the

undeformed configuration is always an equilibrium configuration. As seen in Subsect. XI.2.a, this configuration is stable for $P < \frac{2G}{l}$.

When the value of P is higher than $\frac{2G}{l}$, we conclude from (248) and from Fig. 157c that there are three possible equilibrium configurations: the undeformed configuration which is unstable (point A) and the two roots of (248), θ_1 and $-\theta_1$ (points B and C). These two situations are stable, since an increase of the deformation corresponds to an increase of the load P (positive stiffness). We conclude that the loading capacity of this structure is not exhausted when the critical load corresponding to the undeformed configuration is attained, i.e., this structure has a *stable post-critical behaviour*. Nevertheless, for higher values of P than the critical load, a stable equilibrium requires appreciable deformations, as the diagram in Fig. 157c shows.

The post-critical behaviour of these two structures (Figs 156a and 157a) differs, but they do share a common feature: their behaviour is the same for positive and negative values of the deformation. These structures have a *symmetrical post-critical behaviour*. However, this is not always the case. For example, the third of the structures analysed in Subsect. XI.2.a (Figs. 155d and 158a) has a non-symmetrical behaviour. The relation between angle θ and the corresponding value of P may be obtained in the same way as in the previous two cases.

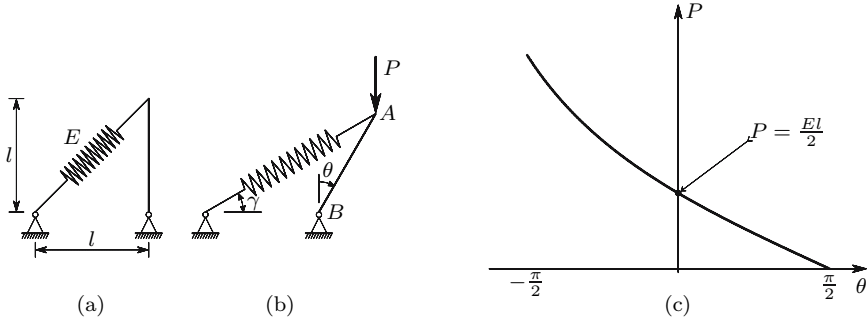


Fig. 158. Non-symmetrical post-critical behaviour

Considering a finite value for the deformation θ (Fig. 158b), relations allowing the computation of P from θ may be obtained

$$\gamma = \arctan \frac{\cos \theta}{1 + \sin \theta} \quad \longrightarrow \quad F_s = El \left(\frac{1 + \sin \theta}{\cos \gamma} - \sqrt{2} \right)$$

$$\longrightarrow \quad P = F_s \frac{\cos \gamma \cos \theta - \sin \gamma \sin \theta}{\sin \theta},$$

where F_s represents the force in the spring. The last expression is obtained by computing the moment of the forces acting in node A , with respect to hinge B , and equating to zero. The relation obtained between P and θ is

represented in Fig. 158c. From this diagram we conclude that the structure has a post-critical behaviour which is unstable for $\theta > 0$ and is stable for $\theta < 0$.

XI.2.c Effect of Imperfections

In the two Sub-sections above, ideal structures have been analysed, that is, the three columns represented in Fig. 155 and the loads P are perfectly vertical and the loads act without any eccentricity on the centroids of the upper cross-sections. Under these conditions, no internal forces are necessary in the deformable elements (the springs) to balance the load P , so the analysis has led to the conclusion that these columns do not deform until the critical load is exceeded.

However, the unavoidable imperfections of the structures may influence their stability behaviour considerably, with respect to the value of the critical load, and even in terms of the characteristics of the deformation. In order to find out about this influence, we analyse the three columns considered in the previous Sub-sections, when they are affected by an imperfection represented by a residual deformation.

Let us first consider the column represented in Fig. 159a which corresponds to the column represented in Fig. 156a with an imperfection represented by the residual deformation α , when P vanishes.

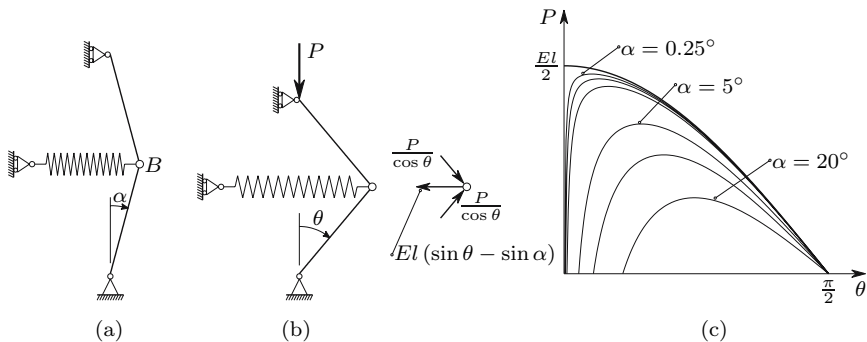


Fig. 159. Effect of an imperfection in a structure with unstable post-critical behaviour

The relation between P and θ may be computed in the same way as in Subsect. XI.2.b. The condition of horizontal equilibrium of the forces acting in node B (Fig. 159b) yields

$$2 \frac{P}{\cos \theta} \sin \theta = El(\sin \theta - \sin \alpha) \Rightarrow P = \frac{El}{2} \overbrace{\frac{\cos \theta (\sin \theta - \sin \alpha)}{\sin \theta}}^{\gamma} . \quad (249)$$

In Fig. 159c curves representing this relation for several values of the imperfection parameter α are represented. We find that, contrary to the column without imperfection, the deformation is present for any value of the load, and that, even small values of the imperfection substantially reduce the maximum value of load the P . This value is given in the following table for the same values of α used in Fig. 159c (γ_{\max} is the maximum value of parameter γ defined in (249)).

α	0°	0.25°	0.5°	1°	5°	10°	20°
γ_{\max}	1.000	0.960	0.937	0.901	0.720	0.572	0.365

If we consider now the second of the structures analysed in Subsect. XI.2.b with an imperfection represented by angle α (Fig. 160a), the equilibrium condition represented by (248) takes the form (Fig. 160b)

$$Pl \sin \theta = 2G(\theta - \alpha) \Rightarrow P = \frac{2G}{l} \frac{\theta - \alpha}{\sin \theta}. \quad (250)$$

Figure 160c shows the curves represented this relation, considering the same values of the imperfection parameter α as in Fig. 159c.

Also in this case we verify that the deformation takes place for any value of the load P . But this deformation suffers a significant increase when P approaches the value corresponding to the critical load of the perfect column. When compared with the column in Fig. 159, the principal difference is that in this case a maximum value of P is not found, even for large values of the imperfection. This difference is a consequence of the fact that this column has a stable post-critical behaviour, while the column in Fig. 159 has unstable behaviour. However, in actual structures the large deformations caused by the imperfection, when the load gets close to the critical value, do limit the loading capacity, even in the case of stable post-critical behaviour, as we will see in Sub-Sects. XI.2.d and XI.4.a.

The analysis of the third column with imperfections may be performed in a similar way. However, since in this case the post-critical behaviour is not symmetric, we must consider imperfections for both sides of the equilibrium configuration. Defining the imperfection by means of the angle α represented in Fig. 161a and using a similar line of reasoning as in the perfect structure (Fig. 158), we arrive at the expressions which allow the computation of the load P corresponding to the deformed configuration defined by angle θ (Fig. 161b)

$$\begin{aligned} \gamma = \arctan \frac{\cos \theta}{1 + \sin \theta} &\longrightarrow F_s = El \left(\frac{1 + \sin \theta}{\cos \gamma} - \frac{1 + \sin \alpha}{\cos \gamma_0} \right) \\ \longrightarrow P = F_s \frac{\cos \gamma \cos \theta - \sin \gamma \sin \theta}{\sin \theta} &\text{ with } \gamma_0 = \arctan \frac{\cos \alpha}{1 + \sin \alpha}. \end{aligned}$$

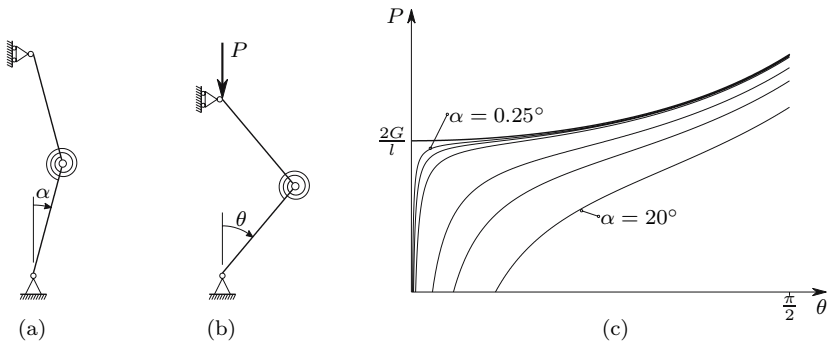


Fig. 160. Effect of an imperfection in a structure with stable post-critical behaviour

From these expressions, using the same values of the imperfection parameter α as in the two previous examples, we get the curves shown in Fig. 161c. We conclude that the effect of the imperfection is similar to that found in the first example (Fig. 159), in the case of positive values of α (unstable post-critical behaviour), while for negative values of the imperfection parameter α the behaviour is similar to that of the second example (Fig. 160 – stable post-critical behaviour).

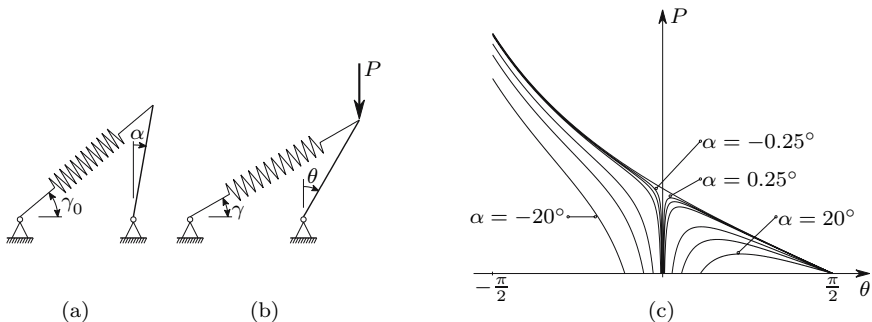


Fig. 161. Effect of an imperfection in a structure with non-symmetrical post-critical behaviour

The analysis expounded in this and the previous Sub-sections illustrates two kinds of structural instability:

- in the perfect structures considered forces are not necessary in the deformed elements, in order to guarantee the equilibrium, so that, before the critical load is reached, no deformation takes place and there is only one equilibrium configuration; when the critical value is attained more than one equilibrium configuration is possible for the same external load; this kind of instability is called *instability by equilibrium bifurcation*;

- in the imperfect structures the deformation appears for any value of the load, suffering a large increase when the load gets close to the critical value of the corresponding perfect structure; in this case, we have the so-called *divergence instability*,¹

XI.2.d Effect of Plastification of Deformable Elements

When the deformable elements of a compressed structure enter the elasto-plastic regime, the corresponding loss of stiffness usually causes a considerable reduction in the maximum load of the structure. In order to get an idea about the importance of this reduction and the conditions under which it occurs, let us consider the example depicted in Figs. 155c and 157a, with the elasto-plastic behaviour of the deformable element – the rotation spring – given by the moment-rotation diagram depicted in Fig. 162.

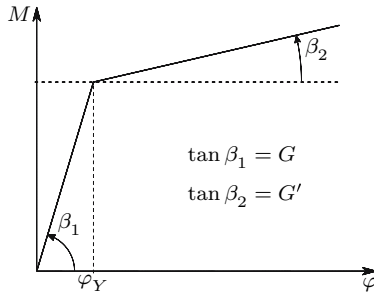


Fig. 162. Elasto-plastic behaviour of the rotation spring in the column represented in Fig. 157a.

If θ is smaller than $\frac{\varphi_Y}{2}$, the relation between θ and the load P is given by (248). When the rotation exceeds the value corresponding to yielding, φ_Y , which happens for higher values of θ than $\frac{\varphi_Y}{2}$ (Fig. 155c), this relation takes the form

$$\theta > \frac{\varphi_Y}{2} \Rightarrow Pl \sin \theta = G\varphi_Y + G'(2\theta - \varphi_Y) \Rightarrow P = \frac{2G}{l} \frac{\frac{\varphi_Y}{2}(1 - \gamma) + \theta\gamma}{\sin \theta},$$

¹This definition is inspired by the small deformation theory where a post-critical analysis is not carried out. For this reason, some authors do not consider this divergence as instability, considering instead another kind of instability called “snap-through”, which corresponds to a vanishing stiffness, as in the imperfect cases depicted in Fig. 159. According to this definition, instability never occurs in the imperfect cases represented in Fig. 160. The definition of divergence instability is retained here, since it is useful in the definition of the point where the interaction between deformation and internal forces becomes important.

with $\gamma = \frac{G'}{G}$. In Fig. 163 the relations between P and θ , described by this equation for $\theta > \frac{\varphi_Y}{2}$ and by (248), for $\theta \leq \frac{\varphi_Y}{2}$, are depicted taking several values of γ and φ_Y .

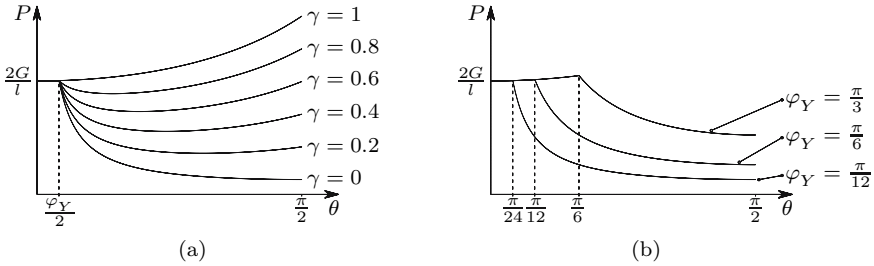


Fig. 163. P - θ relations of the column represented in Fig. 157a, with the constitutivelaw of the rotation spring defined in Fig. 162, for several values of the (a) elasto-plastic stiffness of the spring, $G' = \gamma G$; (b) yielding rotation of the spring, φ_Y , for $\gamma = 0$.

We conclude that yielding transforms the stable post-critical behaviour into unstable, since, after yielding, an increase in the deformation causes a decrease of the corresponding load P . Furthermore, especially for small values of the elasto-plastic stiffness $G' = \gamma G$ and of the yielding rotation of the spring, φ_Y , the failure of the column has the characteristics of a brittle failure, although the behaviour of the spring is ductile. In fact, the yielding of the spring substantially reduces the loading capacity of the column, which practically vanishes when γ and φ_Y take small values.

Since the post-critical behaviour may become unstable when elasto-plastic deformations take place, it is very important to investigate the influence of imperfections on the loading capacity of the column. To this end, let us consider the same column with the imperfection represented by the residual deformation α depicted in Fig. 160a. For smaller values of θ (Fig. 160b) than $\alpha + \frac{\varphi_Y}{2}$ the relation between the load P and the rotation θ is given by (250). For larger deformations the same relation takes the form

$$\begin{aligned} \theta > \alpha + \frac{\varphi_Y}{2} &\Rightarrow Pl \sin \theta = G\varphi_Y + G' [2\theta - (2\alpha + \varphi_Y)] \\ \Rightarrow P &= \frac{2G}{l} \frac{\frac{\varphi_Y}{2} + \gamma(\theta - \alpha - \frac{\varphi_Y}{2})}{\sin \theta} \quad \text{with } \gamma = \frac{G'}{G}. \end{aligned}$$

In Fig. 164 this relation is represented for the particular case of elastic perfectly plastic behaviour ($\gamma = 0$), considering two values for the yielding rotation of the spring, φ_Y , and the same values for the imperfection parameter, α , which have been used in Figs. 159 to 161.

We conclude that even small values of the imperfection cause generally a considerable reduction in the loading capacity of the column. However, in the particular case of a high yielding rotation φ_Y and of a very small value of the

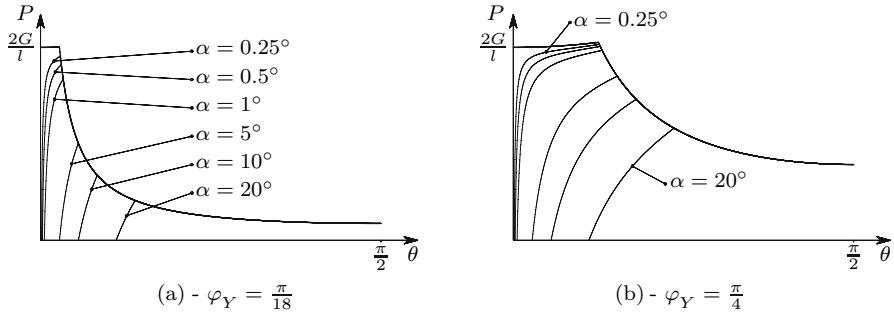


Fig. 164. Effect of an imperfection α , in the case of elastic perfectly plastic behaviour

imperfection parameter α , it is possible to have a maximum load superior to the critical load of the perfect structure ($\frac{2G}{l}$), as shown in Fig. 164-b.

The conclusions reached in relation to the behaviour of the column represented in Fig. 157-a are also valid qualitatively for the case of a compressed prismatic bar, which is of great practical interest and is analysed in the next sections.

XI.3 Instability in the Axial Compression of a Prismatic Bar

XI.3.a Introduction

The main difference between the buckling of an axially compressed prismatic bar and the instability behaviour of the simple examples analysed in Sect. XI.2 is that in the prismatic bar the deformation is distributed throughout the whole bar, while in the simple examples it is concentrated in a single deformable element. Furthermore, those examples have a degree of kinematic indeterminacy of one, which means that only one quantity is needed to define the deformed configuration, while in the prismatic bar the degree of kinematic indeterminacy is infinite, as we will see. As a consequence the analysis of the buckling phenomenon is substantially more complex than the simple examples analysed in Sect. XI.2.

For these reasons, in the analysis presented in the remaining of this Chapter only small deformations are considered, which means that the post-critical behaviour cannot be analysed. However, as mentioned in Subsect. XI.2.a, the buckling of a prismatic bar is qualitatively analogous to the example presented in Figs. 155-c and 157, displaying also a stable post-critical behaviour [11].

XI.3.b Euler’s Problem

Euler has found the critical load of an axially compressed bar by directly analysing the critical state. As we saw in Sect. XI.1 and confirmed in Subject. XI.2.a, in the transition from a stable to an unstable state – the critical state – we have a state of neutral equilibrium, which means that no forces are needed to introduce a small change in the deformation state of the structure. Thus, the critical axial load of a prismatic bar is a force which balances the internal forces (the bending moment, in this case) in a slightly deflected configuration of the bar, without the need of transversal forces, as represented in Fig. 165-a.

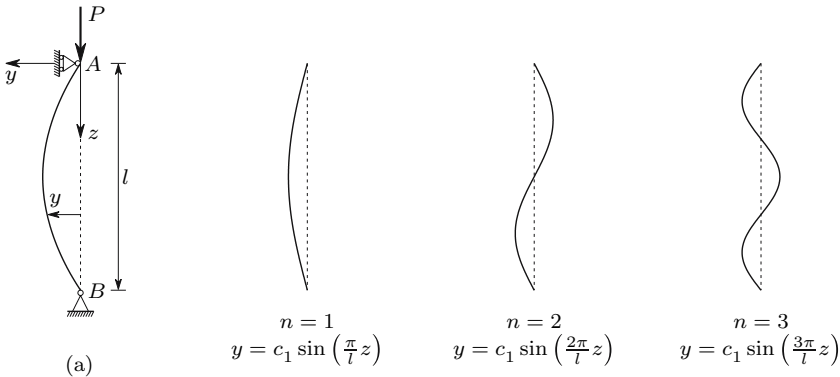


Fig. 165. Euler’s problem: problem definition and buckling shapes

In the deformed configuration depicted in Fig. 165-a the bending moment is given by the expression $M = Py$. Since we are considering only infinitesimal displacements, the rotations will be small. Furthermore, taking only linear elastic material behaviour into consideration, the relation between the bending moment and the deflection y is given by the second of (210). Thus, the deformed configuration of the bar under the conditions represented in Fig. 165-a is given by the solution of the differential equation

$$\left\{ \begin{array}{l} M = Py \\ \frac{|M|}{EI} = \left| \frac{d^2y}{dz^2} \right| \end{array} \right. \Rightarrow Py = -EI \frac{d^2y}{dz^2} \Rightarrow \frac{d^2y}{dz^2} + \frac{P}{EI}y = 0. \quad (251)$$

The minus sign affecting the bending stiffness results from the fact that a positive value of y leads to a negative value of $\frac{d^2y}{dz^2}$ and vice versa. Equation (251) is a linear homogeneous equation with constant coefficients, whose solution takes the form

$$y = C_1 \sin(kz) + C_2 \cos(kz) \quad \text{with} \quad k = \sqrt{\frac{P}{EI}}. \quad (252)$$

The compatibility conditions at the supports yield the relations²

$$\begin{aligned} z = 0 &\Rightarrow y = 0 \Rightarrow C_2 = 0 \\ z = l &\Rightarrow y = 0 \Rightarrow C_1 \sin(kl) = 0 \Rightarrow C_1 = 0 \quad \vee \quad kl = n\pi . \end{aligned} \quad (253)$$

The condition of zero deflection in support B shows that the integration constant C_1 is either zero, or indeterminate ($\sin(kl) = 0$). The first possibility means that the straight configuration is always an equilibrium configuration (although it may be unstable). In the second possibility, the fact that C_1 is indeterminate reflects the fact that the equilibrium is neutral, which means that the amplitude of the deflections does not influence the equilibrium. The last of (253) yields a relation between the load P , the bending stiffness EI and the bar's length l

$$kl = n\pi \Rightarrow k^2 = \frac{n^2\pi^2}{l^2} = \frac{P}{EI} \Rightarrow P = \frac{n^2\pi^2 EI}{l^2} .$$

This expression furnishes an infinite number of values of the axial load P ($n = 1, 2, 3, \dots, \infty$), for which P balances the bending moments in a slightly deflected configuration. The deformed bar has a sinusoidal shape as indicated by (252) ($kl = n\pi$ and $C_2 = 0$). In Fig. 165 these shapes are shown for the three smallest values of n . The critical load is that corresponding to $n = 1$, since it is the minimum value of P which satisfies the necessary (but not sufficient) condition of neutral equilibrium. It may be shown that the configurations corresponding to values of n superior to one are unstable, unless the deflection of the points with $y = 0$ is prevented. The critical load and the corresponding critical stress are then

$$P_{cr} = \frac{\pi^2 EI}{l^2} \Rightarrow \sigma_{cr} = \frac{P_{cr}}{\Omega} = \frac{\pi^2 E}{\lambda^2} \quad \text{with} \quad \lambda = \frac{l}{\sqrt{\frac{I}{\Omega}}} = \frac{l}{i} . \quad (254)$$

The first expression is known as *Euler's formula* and the value P_{cr} as the *Euler buckling load*. The non-dimensional quantity λ is called the *slenderness ratio*. It depends only on the geometry of the bar, represented by the length l and the radius of gyration i of its cross-section. Associated with the modulus of elasticity of the material it completely defines the critical stress.

XI.3.c Prismatic Bars with Other Support Conditions

Equation (254) is only valid for bars with the support conditions shown in Fig. 165-a, i.e., for pin-ended bars. However, in some cases with different support conditions, symmetry considerations allow the generalization of Euler's

²In this analysis the axial deformation does not need to be considered, since the instability is caused by the interaction between the bending deformation and the bending moment caused by the axial force P in a deflected configuration. The axial deformation does not play a role in this interaction.

solution (254), so that the corresponding differential equations do not need to be solved.

In the case of the cantilever represented in Fig. 166-a the critical configuration has the same shape as a pin-ended bar with the length $2l$, which means that the relation between the load P and the bending moment is the same. Thus, the corresponding critical load takes the value

$$P_{cr} = \frac{\pi^2 EI}{(2l)^2} = \frac{\pi^2 EI}{l_e^2} \quad \text{with } l_e = 2l. \tag{255}$$

This value will be confirmed below in the study of the case of composed bending (Subsect. XI.4.a). The quantity l_e is called the *effective length* of the column. It may be defined as the length that a pin-ended bar with the same cross-section would need, in order to have the same critical load as the bar under consideration.

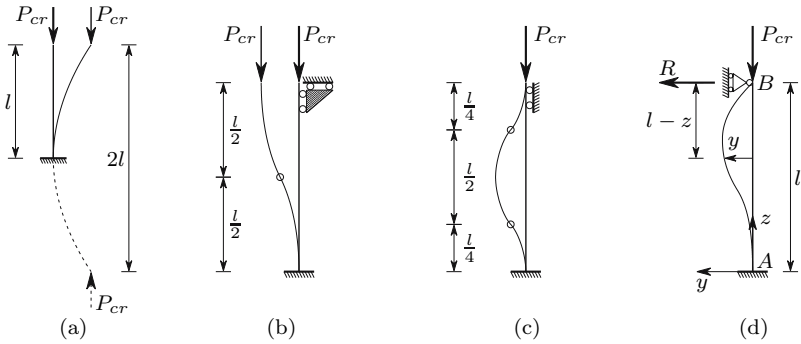


Fig. 166. Determination of effective lengths

Symmetry and antisymmetry considerations easily lead to the conclusion that the effective lengths of the bars represented in Figs. 166-b and 166-c are, respectively $l_e = 2\frac{l}{2} = l$ and $l_e = \frac{l}{2}$.

The critical load of the column represented in Fig. 166-d cannot be obtained from Euler's solution (254), since there are no symmetry or antisymmetry conditions. This load must, therefore, be computed by solving the differential equation of equilibrium in the critical phase, as was done for Euler's problem. To this end, let us consider the reference axes shown in Fig. 166-d. Considering as positive the bending moments corresponding to a positive curvature in this reference system and the reaction force R with the shown direction, we get

$$\begin{cases} M(z) = -Py + R(l - z) \\ \frac{M}{EI} = \frac{d^2y}{dz^2} \end{cases} \Rightarrow \frac{d^2y}{dz^2} + \frac{P}{EI}y = \frac{R}{EI}(l - z).$$

This equation has a homogeneous part which coincides with (251) and admits the particular integral $y = \frac{R}{P}(l - z)$, so that its general solution takes the form

$$y = C_1 \cos(kz) + C_2 \sin(kz) + \frac{R}{P}(l - z) \quad \text{with} \quad k^2 = \frac{P}{EI}. \quad (256)$$

The support conditions in the built-in end A define conditions expressing the integration constants as functions of the reaction force R , yielding

$$z = 0 \Rightarrow \begin{cases} y = 0 \Rightarrow C_1 = -\frac{Rl}{P} \\ \frac{dy}{dz} = 0 \Rightarrow C_2 k - \frac{R}{P} = 0 \Rightarrow C_2 = \frac{R}{Pk}. \end{cases}$$

By substituting these values in the general solution (256) and using the support condition in end B , we get

$$\begin{aligned} z = l \Rightarrow y = 0 \Rightarrow \frac{R}{P} \left[\frac{\sin(kl)}{k} - l \cos(kl) \right] &= 0 \\ \Rightarrow R = 0 \quad \vee \quad \frac{\sin(kl)}{k} - l \cos(kl) = 0 &\Leftrightarrow kl = \tan(kl). \end{aligned} \quad (257)$$

The first possibility, $R = 0$, corresponds to the equilibrium without buckling, since it leads to $y(z) = 0$. The second possibility, $kl = \tan(kl)$, may be used to find the critical load, since it corresponds to a deflected configuration, as R may be different from zero. In this case the value of R is indeterminate, which reflects the fact that the equilibrium is neutral in the critical phase. The value of the critical load may be computed by solving the transcendental equation $kl = \tan(kl)$. The minimum value of kl which satisfies this condition is $kl = 4.493409$. The corresponding critical load may be expressed as a function of an effective length l_e , yielding

$$P_{cr} = EI k^2 = \frac{EI}{l^2} 4.493409^2 = \frac{\pi^2 EI}{\left(\frac{\pi}{4.493409} l \right)^2} = \frac{\pi^2 EI}{l_e^2}$$

$$\text{with} \quad l_e = \frac{\pi}{4.493409} l = 0.6992l \approx 0.7l.$$

Euler's formula may thus be used for this column, provided that an effective length $l_e = 0.7l$ is considered.

The critical load of columns with other support or loading conditions, such as bars with intermediate supports, distributed axial loads, variable cross-section, etc., may be computed by solving the corresponding differential equations (see examples XI.11 to XI.13).

XI.3.d Safety Evaluation of Axially Compressed Members

The theory expounded so far in this Section is valid for a perfectly prismatic bar with a perfectly axial force, i.e., a force whose line of action coincides

with the line defined by the centroids of the cross-sections. Under these conditions, the theory indicates that the bar axis remains straight until the critical load is attained. However, actual members always have imperfections, both in the way the load is applied (eccentricity with respect to the centroid of the cross-sections or inclination with respect to the bar axis) and with respect to the geometry of the bar (residual curvature, non perfectly constant cross-section, etc.). As a consequence of these unavoidable perturbations, the axial force causes bending even when it takes a value which is smaller than the critical load, as shown in the introductory examples with imperfections (Subsect. XI.2.c), and this will be confirmed in the study of the case of bending caused by an eccentric axial force (Sect. XI.4). The bending deformation introduces additional stresses, which become larger when the load gets close to the critical value. As a consequence, the critical load predicted by Euler's formula is usually not reached, since plastic deformations or material failure take place before this point. Residual stresses introduced into the bar by the manufacturing process are also an imperfection, since fibres with a residual compressive stress may reach the limit of proportionality before the computed critical stress (254) is attained, which would influence the value of the critical load (see below).

In addition, as seen in Subsect. XI.2.d, the buckling failure of a bar has the characteristics of a brittle failure, since its axial strength after buckling is practically reduced to zero, even in the case of ductile material behaviour.

For these two reasons, in the safety evaluation of long members (bars in which Euler's critical stress is smaller than the proportionality limit stress) by means of Euler's formula, a supplementary safety coefficient, ψ , is used. Thus, in the design of long axially compressed bars, the following condition must be satisfied:

$$P \leq \frac{\pi^2 EI}{\psi l_e^2} \Rightarrow \sigma \leq \frac{\pi^2 E}{\psi \lambda^2} .$$

Coefficient ψ is usually considerably greater than one. A current value is $\psi = 1.8$.

In the case of columns with intermediate slenderness, i.e., bars which are stable for stresses higher than the proportionality limit, Euler's theory may still be used, provided that the tangent modulus of elasticity corresponding to the critical stress is used. Since this stress itself depends on the elasticity modulus, Euler's critical load must be computed by means of an iterative approach (see example XI.16). In order to avoid this process, and also because it is not easy to define the exact value of the tangent modulus of elasticity, the safety of columns with intermediate slenderness is commonly evaluated by means of experimentally obtained curves which give the critical buckling stress as a function of the slenderness ratio.

In the case of steel structures, the so-called Tetmeyer's line is often recommended, especially in the codes of European countries. Tetmeyer has approximated by straight lines the experimental results for the relation between the slenderness ratio and critical stress in columns with intermediate slenderness.

These lines pass through the point where Euler's theory ceases to be valid, i.e., the point whose ordinate is the proportionality limit stress. For very low values of the slenderness ratio (short columns) this line may give results which are higher than the yielding stress of the material, so that Tetmeyer's line is not applicable to such columns. In these cases there is no buckling failure, which means that the limit stress is the maximum allowable stress for the material under consideration.

As an alternative to the Tetmeyer's line, an approximation by means of a parabola, known as Johnson's parabola, is also used. This curve has a vanishing tangent at the point corresponding to zero slenderness ($\lambda = 0, \sigma_{cr} = \sigma_Y$), is tangent to the hyperbola defined by Euler's theory $\sigma_{cr} = \frac{\pi^2 E}{\lambda^2}$ and is valid for columns with a lower slenderness than that corresponding to the contact point between these two curves. It may easily be verified that the coordinates of this point are $\lambda = \pi \sqrt{\frac{2E}{\sigma_Y}}$ and $\sigma_{cr} = \frac{\sigma_{all}}{2}$ and that the parabola has the equation

$$\sigma_{cr} = \sigma_Y - \frac{\sigma_Y^2}{4\pi^2 E} \lambda^2 .$$

Figure 167 gives the two approximations. When used for safety evaluation, the values defined by these curves must be affected by safety coefficients which, as mentioned above, should have higher values in the case of long members.

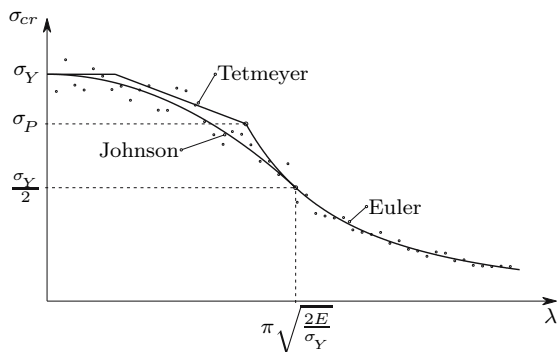


Fig. 167. Approximation of experimental values in axially compressed members
 experimental — results

In the case of Tetmeyer's approximation, it is usually considered that for slenderness ratios below 20 there is no buckling failure. The Tetmeyer's straight line is thus used for slenderness ratios between 20 and the value corresponding to the limit of proportionality, σ_p , which depends on the steel type under consideration. A value of $\sigma_p \approx 0.8\sigma_Y$ is considered in some codes, which leads to the following values of the slenderness ratio

$$\frac{\pi^2 E}{\lambda^2} = 0.8 \sigma_Y \Rightarrow \lambda = \pi \sqrt{\frac{E}{0.8 \sigma_Y}} \Rightarrow \begin{cases} \lambda = 105 (S 235) \\ \lambda = 96 (S 275) \\ \lambda = 85 (S 355) \end{cases},$$

where $S 235$, $S 275$ and $S 355$ are current steel grades, which have the nominal yielding stresses of 235, 275 and 355 MPa , respectively. These considerations are summarized in the design curves represented in Fig. 168.

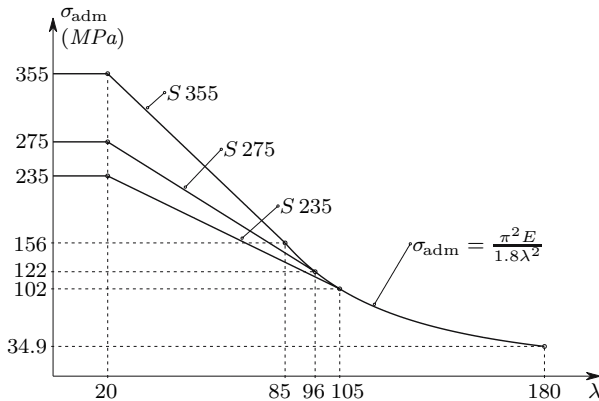


Fig. 168. Design curves for axial compression for current steel grades ($\psi = 1.8$)

From these curves we conclude that the use of high-strength steel in bars with a larger than 105 slenderness ratio does not increase the loading capacity. This is because the only material parameter entering Euler's formula is the modulus of elasticity E which takes the same value for all steel grades.

If the bar has the same effective length in both principal bending planes, buckling takes place by bending around the principal axis of inertia with the lowest value of the moment of inertia, since the maximum slenderness corresponds to the minimum value of the radius of gyration (254). However, very often the effective length is not the same in the two principal bending planes, and the smallest effective length corresponds to the smallest moment of inertia. In these cases buckling takes place in the bending plane with the highest slenderness ratio (see example XI.8).

If the cross-section of the column does not have two symmetry axes, the centroid and the shear centre will have distinct positions. In these cases, buckling may be accompanied by torsion, especially in bars with a small torsional stiffness, such as open thin-walled cross-sections. This torsional effect is due to small inclinations of the axial force with respect to the bar axis causing a small shear force which induces torsion because it does not pass through the shear centre.

There is also the possibility of torsional buckling, even in the case of doubly symmetric cross-sections. This kind of instability may occur in columns with

very thin cross-section walls and higher bending stiffness. The general study of these phenomena is beyond the scope of this text, however, because it is a relatively complex analysis which has no practical relevance, since, in usual cross-sections, bending instability occurs before torsional instability. However, an example of the computation of the torsional buckling load in a cruciform cross-section is included (see example XI.15).

XI.3.e Optimal Shape of Axially Compressed Cross-Sections

From what has been explained above, we conclude that in most cases buckling takes place by bending around the principal axis of inertia which corresponds to the highest value of the slenderness ratio. If the cases with very different effective lengths in the two principal bending planes are excluded, we conclude that, in order to get high values of buckling strength, high flexural stiffness in both principal bending planes is required. Since the material around the centroid of the cross-section makes a lower contribution to the bending stiffness, the cross-section of compressed members should have the most part of the area far from the centroid and should have similar values in the two principal moments of inertia. Furthermore, torsional effects in buckling may be avoided by giving the cross-section a high torsional stiffness. A closed thin-walled cross-section, such as a square or circular tube, satisfies all of these conditions.

XI.4 Instability Under Composed Bending

XI.4.a Introduction and General Considerations

Instability phenomena under composed bending with a compressive axial force may be analysed using the same tools as in the case of purely axial compression. There is, however, a much larger variety of differential equations to be solved, since a distinct equation is obtained for each kind of transversal displacement. For this reason, alternative, generally semi-empirical, expressions are frequently used in the safety evaluation of compressed and bent members. However, before some of those alternative expressions are presented, we first analyse in detail a particular case of composed bending with compressive axial force, in order to facilitate the physical understanding of the phenomenon of interaction between deformation and internal forces.

Let us consider the cantilever column represented in Fig. 169 which is eccentrically compressed by a force P . The differential equation expressing the interaction between the deformation and the bending moment may be obtained from the relations between bending moment and curvature and between bending moment and deflection. Considering only small rotations, we have

$$\begin{cases} M = P(\delta + e - y) \\ M = EI \frac{d^2 y}{dz^2} \end{cases} \Rightarrow \frac{d^2 y}{dz^2} + k^2 y = k^2(\delta + e) \quad \text{with} \quad k^2 = \frac{P}{EI}. \quad (258)$$

This equation admits the particular integral $y = \delta + e$ and has the same homogeneous solution as (251). The general solution is then

$$y = C_1 \sin(kz) + C_2 \cos(kz) + \delta + e.$$

The integration constants are computed from the support conditions in cross-section A , yielding

$$z = 0 \Rightarrow \begin{cases} y = 0 \Rightarrow C_2 = -\delta - e \\ \frac{dy}{dz} = 0 \Rightarrow C_1 = 0 \end{cases} \Rightarrow y = (\delta + e)[1 - \cos(kz)].$$

The relation between the maximum deflection δ and load P is then

$$z = l \Rightarrow y = \delta = (\delta + e)[1 - \cos(kl)] \Rightarrow \delta = e \frac{1 - \cos(kl)}{\cos(kl)}. \quad (259)$$

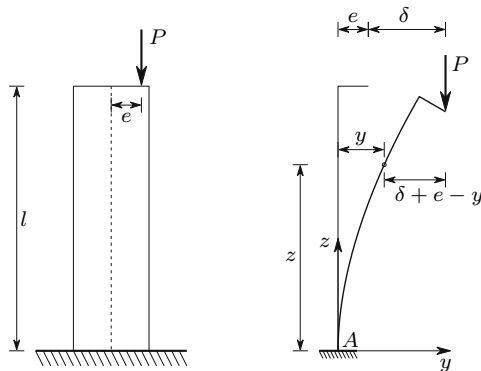


Fig. 169. Eccentric compression of a column

We conclude that when kl reaches the value $\frac{\pi}{2}$ the displacement δ becomes infinite. This means that the critical load has been attained, since the column has lost stiffness to oppose the bending moment caused by load P . In the case of Euler's problem this bending moment vanishes, and so we have neutral equilibrium in the critical phase. Remembering the analogy with the example of the sphere (Fig. 154), this situation corresponds to having a small horizontal force applied to the sphere: in the stable situation this force causes a small displacement in relation to the point with zero slope; in the critical situation (Fig. 154-c) this force would cause an infinite displacement. This

kind of instability, where the deformation gradually increases, going to infinite values when the load attains the critical load, corresponds to the divergence instability which has been defined at the end of Subsect. XI.2.c. The fact that an infinite deformation is obtained for $P = P_{cr}$ is a consequence of the assumption of small rotations, which actually makes a post-critical analysis impossible. As seen above, in the perfect bars under perfectly axial loading there is no deformation until the critical load is attained. When this happens, there is equilibrium in both the undeformed and slightly deformed configurations. In this case we have the bifurcation instability defined in Subsect. XI.2.c. As already mentioned (Subsect. XI.2.c), actual columns always exhibit divergence instability, since imperfections are unavoidable.³

The critical load is then

$$kl = \frac{\pi}{2} \Rightarrow P_{cr} = \frac{\pi^2 EI}{(2l)^2}.$$

This value coincides with that given by (255), which means that the bending moment introduced by the eccentricity of the load does not influence the critical load. This conclusion may be generalized to other loading cases, since, with the exception of the cases where the applied loads depend on the deformation (non-conservative loads), the bending moment only influences the particular solution of the differential equation, while the critical load is determined by $\sin(kz)$ or $\cos(kz)$, which appear in the solution of the homogeneous equation. A physical interpretation of the same phenomenon is that there is no interaction between this bending moment and the deformation, that is, the deformation does not increase the additional bending moment introduced by the eccentricity of the axial load.

In composed bending with a compressive axial force the maximum applicable load is always smaller than the critical load, even in the case of long members, since, as a consequence of the additional stresses introduced by bending, the maximum allowable stress is reached before the load attains the critical value. The maximum stress introduced by eccentric loading may be computed by means of the so-called *secant formula*, which is obtained from (259), yielding

$$\begin{cases} M_{\max} = P(\delta + e) = \frac{Pe}{\cos(kl)} \\ \sigma_{\max} = \frac{P}{\Omega} + \frac{M_{\max}}{I} \end{cases} \Rightarrow \sigma_{\max} = \frac{P}{\Omega} + \frac{Pe}{I \cos(kl)}. \quad (260)$$

We conclude that the interaction between the bending moment and the deformation causes an increase in the stress caused by bending which is represented by the factor $\frac{1}{\cos(kl)} = \sec(kl)$.⁴

³If we take $e = 0$ in (259) (purely axial loading), we also get an indeterminate value for the deflection δ , if $kl = n\frac{\pi}{2}$.

⁴The stresses caused by the axial force and by the bending moment may be computed separately and added together, although the superposition principle, in its

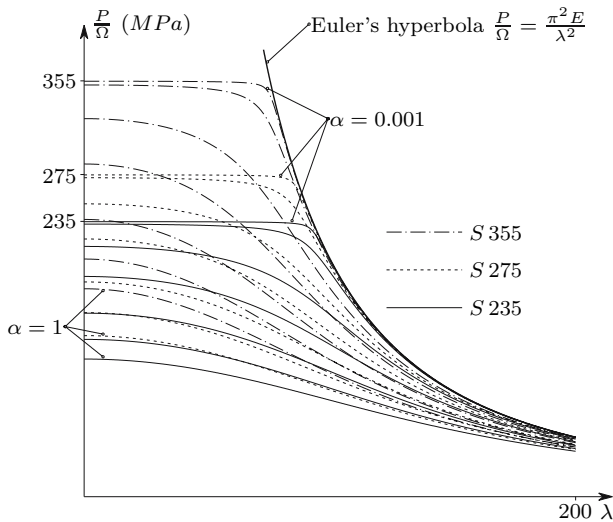


Fig. 170. Eccentric axial loads which may be applied to steel columns for several values of the eccentricity ratio α . $\alpha=0.001$ $\alpha=0.01$ $\alpha=0.1$ $\alpha=0.25$ $\alpha=0.5$ $\alpha=0.75$ $\alpha=1$

The maximum value of the eccentric load P , for a given value of the allowable stress, σ_{all} , may be related to the slenderness ratio of the bar. This relation may be obtained from (260), yielding

$$\left\{ \begin{array}{l} kl = \sqrt{\frac{Pl^2}{EI}} = \sqrt{\frac{Pl_e^2}{4E\Omega i^2}} = \sqrt{\frac{\lambda^2 P}{4E \Omega}} \\ \sigma_{max} = \sigma_{all} \end{array} \right. \Rightarrow \left| \begin{array}{l} \frac{P}{\Omega} + \alpha \frac{\frac{P}{\Omega}}{\cos \sqrt{\frac{\lambda^2 P}{4E \Omega}}} = \sigma_{all} \\ \text{with } \alpha = \frac{ve}{j^2} . \end{array} \right. \quad (261)$$

The relation between $\frac{P}{\Omega}$, λ and σ_{all} depends on the eccentricity of the load which is expressed by the non-dimensional parameter α , called the *eccentricity ratio*. By ascribing fixed values to α and σ_{all} , a relation between λ and $\frac{P}{\Omega}$ is obtained. This is actually a transcendental equation, so an explicit expression for $\frac{P}{\Omega}$ cannot be found. The value of $\frac{P}{\Omega}$ corresponding to a given value of λ may, however, be obtained by numerical means using, for example, the Newton-Raphson algorithm. This has been done for the three steel grades considered above (Fig. 168), yielding the results represented by the curves depicted in Fig. 170.

most general form, cannot be applied when the interaction between internal forces and deformations is taken into account. In fact, the non-linearity of the problem appears in the relation between external and internal forces (P and M_{max} in this case) and not in the relation between internal forces and stresses.

From these curves we conclude that, when the eccentricity goes to zero, the load capacity of the column tends to the value defined by Euler's formula, if the corresponding critical stress is smaller than the maximum allowable stress σ_{all} (i.e., if $\frac{\pi^2 E}{\lambda^2} \leq \sigma_{\text{all}}$), while in less slender columns it tends to the maximum allowable stress of the steel grade under consideration. Obviously, these curves do not take into consideration the fact that the proportionality limit stress may be smaller than the maximum allowable stress.

The maximum deflection δ may be expressed as a function of the ratio between the applied and the critical loads, $\frac{P}{P_{cr}}$, and of the eccentricity e . From (259), we get

$$kl = \sqrt{\frac{Pl^2}{EI}} = \sqrt{P \left(\frac{\pi}{2}\right)^2 \frac{(2l)^2}{\pi^2 EI}} = \frac{\pi}{2} \sqrt{\frac{P}{P_{cr}}} \Rightarrow \delta = e \frac{1 - \cos\left(\frac{\pi}{2} \sqrt{\frac{P}{P_{cr}}}\right)}{\cos\left(\frac{\pi}{2} \sqrt{\frac{P}{P_{cr}}}\right)}.$$

Dividing both members of this expression by the length of the column, l , the non-dimensional relations depicted in Fig. 171-a are obtained.

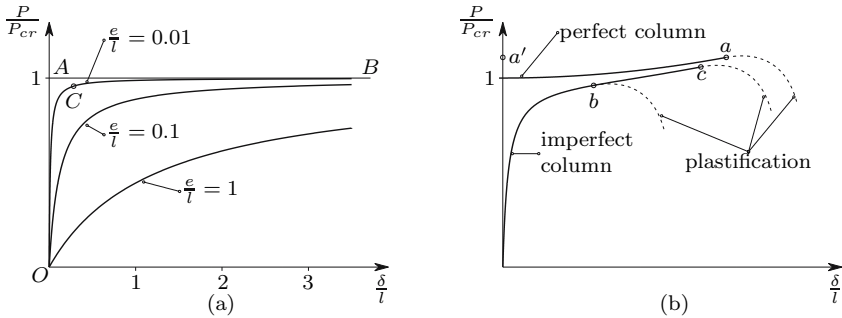


Fig. 171. Deformations caused by an eccentric compression: (a) infinitesimal rotations (b) finite rotations

The maximum value of the stress is attained when the deflection δ , reaches a certain value, since $M = P(\delta + e)$. The diagrams in Fig. 171-a show that, for a small eccentricity, the load-displacement curve is very close to Euler's solution (line OAB) and that the maximum allowable load gets very close to Euler's critical load (point C in the diagram).

Furthermore, we must remember that the differential (258) has been established under the condition of infinitesimal rotations. The exact equation⁵

⁵The equation obtained without the restriction to infinitesimal rotations contains, in the place of the second derivative of y with respect to z , the curvature expression defined in (208) or (215). The solution of this equation may be found in reference [11]. This solution has been obtained by means of a Lagrangian formulation of the problem (see Footnote 61 in Chap. IX).

yields the solution represented in a qualitative approach in Fig. 171-b. From this curve we conclude that in a perfect column (that is, without eccentricity) the maximum allowable load is always higher than Euler's critical load (point a on the diagram). This is due to the fact that an elastic column exhibits stable post-critical behaviour (note the similarity between the curves represented in Fig. 171-b and the curves depicted in Fig. 160-c).

The imperfect column generally reaches the maximum allowable stress before the load attains the critical value, as mentioned above (point b on the diagram). However, in the same way as in the simple example analysed in Subsect. XI.2.d, if the column is flexible enough and if the imperfections are small, it may withstand a higher axial force than Euler's critical load, even with a small eccentricity (point c on the diagram).

In the same way as in the second of the simple examples analysed in Subsect. XI.2.b, the bifurcation of the equilibrium state which occurs in the perfect bar, when the load exceeds the critical value, becomes more clear in the case of finite deformations. From Fig. 171-b we conclude that for higher loads than the critical value, there are two equilibrium configurations: one, corresponding to the undeformed configuration of the column (point a') is unstable; the other is stable and corresponds to the deformed configuration represented by the abscissa of point a .

XI.4.b Safety Evaluation

Expressions of the type of (260) might be found for other loading cases (see example XI.14). Some of these solutions are given in reference [3]. In the case of inclined bending, the expression of the stress will have another term, corresponding to the other principal bending moment. In the case of eccentric compression with respect to the two principal axes of inertia of the cross-section, (260) is replaced by the following expression (e_x and e_y are the eccentricities with respect to the principal axes)⁶

$$\sigma_{\max} = \frac{P}{\Omega} + \frac{Pe_x}{\left(\frac{I}{v}\right)_x \cos(k_x l)} + \frac{Pe_y}{\left(\frac{I}{v}\right)_y \cos(k_y l)} \quad \text{with} \quad \begin{cases} k_x^2 = \frac{P}{EI_x} \\ k_y^2 = \frac{P}{EI_y} \end{cases} .$$

⁶A cross-section with a rectangular convex contour and a symmetry axis is assumed when the section moduli with respect to the principal axes x and y , are used.

It should be noted that both this expression and (260) are deduced without using the superposition principle, since this principle is not valid when the interaction between deformation and internal forces is taken into account, although the linear analysis of composed bending (155) has been carried out on the basis of that principle. In axial compression that is eccentric with respect to the two principal axes of the cross-section, two independent equations of the type of (258) are established. Thus, they may be solved separately, yielding the results $\delta_x = e_x \frac{1 - \cos(k_x l)}{\cos(k_x l)}$ and $\delta_y = e_y \frac{1 - \cos(k_y l)}{\cos(k_y l)}$ for the displacements of the upper end of the cantilever column in directions y and x , respectively.

When expressions like this are used in the safety evaluation, the following three points must be taken into consideration:

- A semi-probabilistic approach (Subsect. V.9.d) should be used, that is, the load is multiplied by a factor, instead of a safety coefficient being used for the stresses, since they are not proportional to the load.
- These expressions are valid only in the linear elastic phase, i.e., only if the stresses do not exceed the proportionality limit, and lead to an overestimation of the safety degree (that is, the error is disadvantageous to safety), when they are used above this limit.
- When the eccentricity vanishes, only the term $\sigma = \frac{P}{\Omega}$ remains, which obviously does not take the buckling risk into account. For this reason a residual eccentricity in both principal bending planes shall be considered, which corresponds to considering imperfections in how the load is applied or in the geometry of the column. As an alternative, the methods described in Subsect. XI.3.d for axially compressed members may of course be used.

As mentioned at the beginning of this Section, semi-empirical expressions are often used in the safety evaluation of compressed and bent members. The more straightforward ones are based on the generalization of the linear expression for composed bending, (155), using the so-called *buckling coefficient*. This coefficient is defined as the ratio between the maximum allowable stress in axial compression, σ_{adm} (Fig. 168) and the nominal value of the allowable stress for the material the bar is made of, σ_{all} , that is

$$\varphi = \frac{\sigma_{\text{adm}}}{\sigma_{\text{all}}} \leq 1 .$$

The simplest equation limits the value of the maximum stress to the value obtained by multiplying the nominal value of the allowable stress defined for the material by the buckling coefficient, which leads to the expression

$$\frac{P}{\Omega \varphi \sigma_{\text{all}}} + \frac{M_x}{\left(\frac{I}{v}\right)_x \varphi \sigma_{\text{all}}} + \frac{M_y}{\left(\frac{I}{v}\right)_y \varphi \sigma_{\text{all}}} \leq 1 .$$

However, in bars with a large bending moment and a small axial force, this expression leads to exaggerated dimensions, since instability is caused only by the interaction between the moment caused by the axial force and the bending deformation. In these cases, the so-called *interaction formula* may be used, in which the buckling coefficient affects only the term corresponding to the axial force, yielding

$$\frac{P}{\Omega \varphi \sigma_{\text{all}}} + \frac{M_x}{\left(\frac{I}{v}\right)_x \sigma_{\text{all}}} + \frac{M_y}{\left(\frac{I}{v}\right)_y \sigma_{\text{all}}} \leq 1 .$$

It must be noted that this approximate expression may overestimate the loading capacity of the bar (see example XI.17).

In the design codes for metallic structures more elaborate expressions are usually given, which take into account the way the bar is connected to the rest of the structure, the risk of lateral buckling (buckling of the compressed part of a bent beam), etc., as well as design rules for avoiding local instability of elements of profile cross-sections, such as web and flanges.

XI.4.c Composed Bending with a Tensile Axial Force

In the case of a tensile axial force, the interaction between internal forces and deformations (second-order effects) may be analysed with the same tools described above for the case of compression. The results obtained are similar, with the difference that hyperbolic functions appear in place of trigonometric functions ($\sinh(kz)$ and $\cosh(kz)$ instead of $\sin(kz)$ and $\cos(kz)$). Obviously, there are no critical loads, since these hyperbolic functions never vanish when the argument is other than zero.

From a physical point of view, it is obvious that the interaction between the bending moment caused by the axial force and the bending deformation reduces this deformation and, as a consequence, the stresses caused by bending. Thus, the error introduced when the second-order effects are not taken into account is advantageous for safety, since larger stresses than the actual ones are computed. For this reason, the second-order effects are usually not considered, when the safety of members under composed bending with a tensile axial force is analysed.

When the global critical load of framed structures, where tensile axial forces appear, is to be computed, the beneficial effects of the tensile internal forces on global stability shall be considered, in order to get an accurate estimate for that load. In Sect. XI.6 a global stability analysis of framed structures using the displacement method is introduced, which takes the influence of the tensile forces in the bending stiffness into account.

XI.5 Examples and Exercises

XI.1. Determine the critical loads of the plane structures represented in Figs. XI.1-a to XI.1-d.

Resolution

- (a) The critical load may be obtained from the equilibrium condition between the applied load and the forces in the springs in a slightly deformed configuration, as depicted in Fig. XI.1-e.

Considering that the deformation represented by angle θ is infinitesimal, and disregarding higher order infinitesimal quantities, the moment balance condition with respect to point A (Fig. XI.1-e), yields

$$P_{cr} \times \theta l = E\theta l \times l \Rightarrow P_{cr} = El .$$

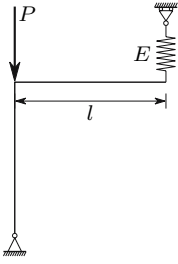


Fig. XI.1-a

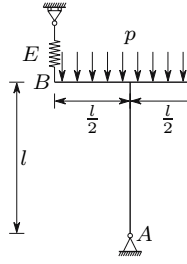


Fig. XI.1-b

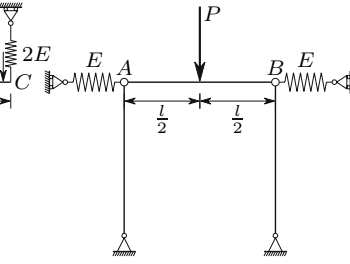


Fig. XI.1-c

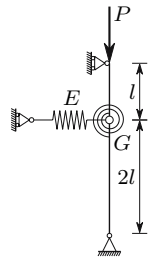


Fig. XI.1-d

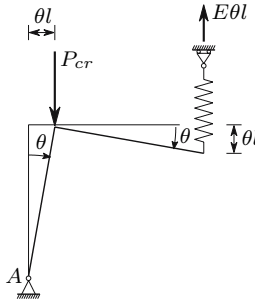


Fig. XI.1-e

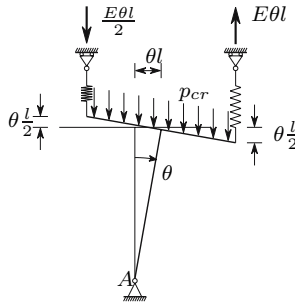


Fig. XI.1-f

(b) The critical load of this structure may be computed in the same way as the previous one. The condition of moment balance with respect to point A leads to (Fig. XI.1-f)

$$\begin{aligned}
 p_{cr} l \times \theta l &= \frac{E\theta l}{2} \times \frac{l}{2} + E\theta l \times \frac{l}{2} \\
 \Rightarrow p_{cr} &= \frac{3}{4} E .
 \end{aligned}$$

(c) In this structure the critical load may be computed by means of the horizontal balance condition of the forces acting on bar AB. From Fig. XI.1-g

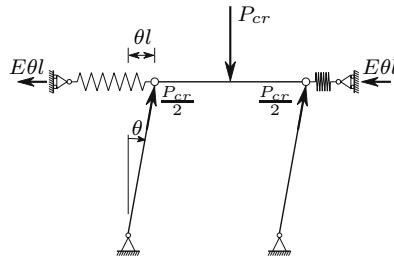


Fig. XI.1-g

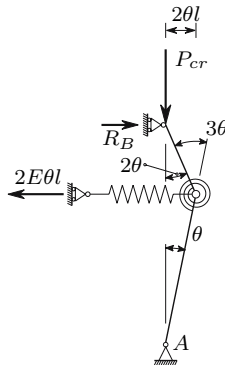


Fig. XI.1-h

we conclude that, for an infinitesimal value of θ , this condition may be expressed by

$$2E\theta l = 2 \frac{P_{cr}}{2} \theta \Rightarrow P_{cr} = 2El .$$

- (d) The critical load of this structure may also be computed by means of the balance conditions of the forces acting on the structure in the deformed configuration defined by angle θ (Fig. XI.1-h). The moment balance condition with respect to point A yields the value of the reaction force in support B (the elongation of the spring is $2\theta l$)

$$R_B \times 3l = 2E\theta l \times 2l \Rightarrow R_B = \frac{4}{3}E\theta l .$$

The critical load may then be computed by means of the bending moment needed to introduce a rotation 3θ into the rotation spring. Expressing this moment as a function of the forces acting on node B , we get

$$P_{cr} \times 2\theta l - \frac{4}{3}E\theta l \times l = 3\theta G \Rightarrow P_{cr} = \frac{3}{2} \frac{G}{l} + \frac{2}{3}El .$$

XI.2 Consider the mechanism represented in Fig. XI.2-a under the action of forces p and F . The stability of this structure depends on the value of

force F . Considering the pin-ended bars as axially rigid, determine the minimum value of force F , in order to have a stable structure.

Resolution

This problem may be solved with the same line of reasoning that was used in problem XI.1. Thus, since in the critical situation an infinitesimal perturbation does not disturb the equilibrium, we may find the minimum value of force F by means of equilibrium considerations in the forces acting on the mechanism, when it suffers the perturbation defined by the infinitesimal angle θ (Fig. XI.2-b). The horizontal balance condition of the forces acting in bars AB and BC yields

$$4\frac{pl}{2} \times \theta = F_{\min} \times \frac{2}{3}\theta \Rightarrow F_{\min} = 3pl .$$

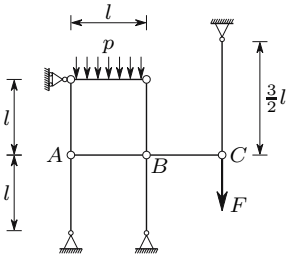


Fig. XI.2-a

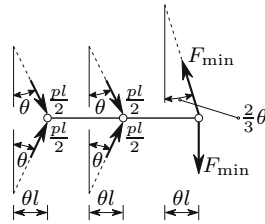


Fig. XI.2-b

XI.3 Find the relation between the lengths l and l' , so that the mechanism represented in Fig. XI.3-a is stable.

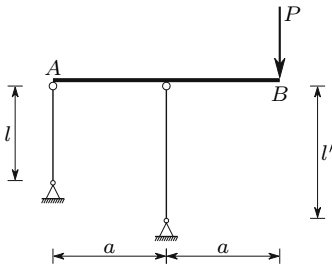


Fig. XI.3-a

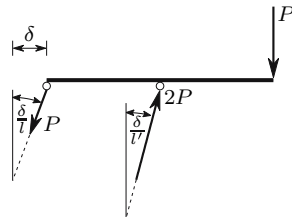


Fig. XI.3-b

Resolution

Also in this case the stability analysis may be performed by means of the horizontal balance condition of the forces acting on bar AB in a slightly disturbed configuration. Thus, considering the perturbation defined by the infinitesimal displacement δ , we conclude that the tensile axial force in the left pin-ended bar, P , opposes the perturbation, while the compressive force $2P$ in the right vertical bar has a component which tends to increase the perturbation. Therefore, the structure will be stable if the horizontal component of the tensile force is greater than the horizontal component of the compressive force, that is

$$P \frac{\delta}{l} \geq 2P \frac{\delta}{l'} \Rightarrow l' \geq 2l .$$

We conclude that the stability of this structure does not depend on the value of P , which is a consequence of the fact that the structure does not have deformable elements opposing the deformation.

XI.4 In the structure represented in Fig. XI.4-a, load P may be displaced along the beam. Without considering any deformation in the bars, determine the region of the beam where the load may be to have a stable situation.

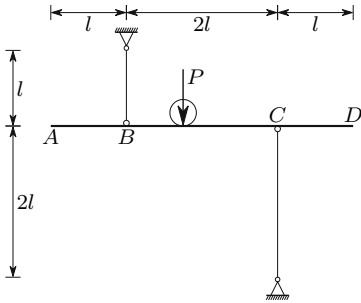


Fig. XI.4-a

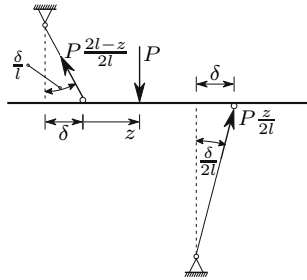


Fig. XI.4-b

Resolution

When the load P is on beam segment AB , the structure is stable, since the two vertical bars have tensile axial forces. But if load P is on beam segment CD , the equilibrium is unstable, since both vertical bars have compressive axial forces. If the load is in segment BC , the structure will be stable if the stabilizing force introduced by the tensile axial force in the left vertical bar is larger than the destabilizing force corresponding to the compressive axial force in the right vertical bar. Thus, considering the infinitesimal perturbation δ represented in in Fig. XI.4-b, we conclude that stability requires the following condition to be satisfied

$$P \frac{2l - z}{2l} \frac{\delta}{l} > P \frac{z}{2l} \frac{\delta}{2l} \Rightarrow 2l - z > \frac{z}{2} \Rightarrow z < \frac{4}{3}l \approx 1.333l .$$

Thus, the structure will be stable if the load is on beam segment AB , or in beam segment BC at a smaller distance than $1.333l$ of point B .

XI.5 Determine the critical load of the structure represented in Fig. XI.1-b, supposing that the load p remains perpendicular to bar BC .

Resolution

Under these conditions, the structure is stable for any value of p , since the equilibrium between load p and the reaction force in support A is not affected by a perturbation like that represented in Fig. XI.1-f.

XI.6 Determine the critical load of the structure represented in Fig. XI.6.

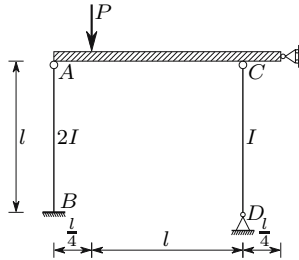


Fig. XI.6

Resolution

Buckling failure of this structure takes place when one of the vertical bars buckles. Since the horizontal displacements in points A and C are prevented, there is no interaction between the two vertical bars, that is, they buckle independently of each other. Therefore, the critical load is the smallest of the two values of P which correspond to the critical axial force in each column. Taking the different effective lengths, support conditions and moments of inertia into consideration, the critical axial forces of the two columns are

$$N_{cr}^{AB} = \frac{\pi^2 E 2I}{(0.7l)^2} = \frac{2}{0.7^2} \frac{\pi^2 EI}{l^2}; \quad N_{cr}^{CD} = \frac{\pi^2 EI}{l^2} .$$

Since the reaction forces in the supports B are D $\frac{4}{5}P$ and $\frac{1}{5}P$, respectively, the values of P which correspond to these two axial forces are, respectively

$$\frac{4}{5}P = \frac{2}{0.7^2} \frac{\pi^2 EI}{l^2} \Rightarrow P = 5.102 \frac{\pi^2 EI}{l^2}; \quad \frac{1}{5}P = \frac{\pi^2 EI}{l^2} \Rightarrow P = 5 \frac{\pi^2 EI}{l^2} .$$

The critical load of this structure is the smallest of these two values, i.e., $P_{cr} = 5 \frac{\pi^2 EI}{l^2}$.

XI.7 Determine the increase of buckling strength that is obtained in the structure represented in Fig. XI.7 when a support is added which prevents the horizontal displacement of point A .

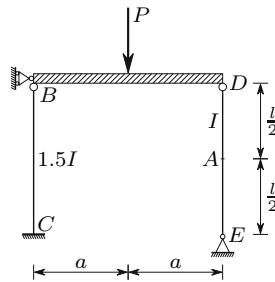


Fig. XI.7

Resolution

In the original situation (without the support in A) the right vertical buckles at first. The corresponding value of force P is

$$N_{DE} = \frac{P}{2} = \frac{\pi^2 EI}{l^2} \Rightarrow P = 2 \frac{\pi^2 EI}{l^2} .$$

When the horizontal displacement of point A is prevented, the first buckling mode (Fig. 165, $n = 1$) cannot occur. Thus, the critical axial force of the bar is that corresponding to the second mode (see Fig. 165 with $n = 2$ and example XI.13), that is, $N_{cr} = \frac{4\pi^2 EI}{l^2}$. Under these conditions, the values of P corresponding to the critical axial forces in each column are

$$N_{BC} = N_{cr}^{BC} \Rightarrow \frac{P}{2} = \frac{\pi^2 E 1.5I}{(0.7l)^2} \Rightarrow P \approx 6.122 \frac{\pi^2 EI}{l^2}$$

$$N_{DE} = N_{cr}^{DE} \Rightarrow \frac{P}{2} = \frac{4\pi^2 EI}{l^2} \Rightarrow P = \frac{8\pi^2 EI}{l^2} .$$

Since the critical load of the structure is the smallest of these two values, we conclude that the horizontal support in point A raises the critical load from $2 \frac{\pi^2 EI}{l^2}$ to $6.122 \frac{\pi^2 EI}{l^2}$.

XI.8 The column of the structure represented in Fig. XI.8 has a rectangular cross-section, with the dimension a in the plane of the structure and $2a$ in the perpendicular direction. The displacement of point A in the direction perpendicular to the structure's plane is not prevented. Determine the critical load of this structure.

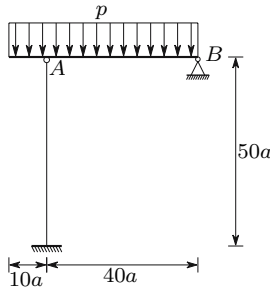


Fig. XI.8

Resolution

The column may buckle in the plane of the structure, with the buckling shape depicted in Fig. 166-d, since the beam prevents the displacement of point A in direction AB . Another possibility is buckling in the perpendicular plane with the buckling shape depicted in Fig. 166-a. Of these two possibilities, the actual buckling mode is that corresponding to the smallest value of the slenderness ratio. In the first case, we have, since the cross-section has a height $h = a$ and a width $b = 2a$

$$\begin{cases} i^2 = \frac{I}{\Omega} = \frac{2a \times a^3}{12} \times \frac{1}{2a^2} = \frac{a^2}{12} \\ l_e = 0.7l = 0.7 \times 50a = 35a \end{cases} \Rightarrow \lambda = \frac{l_e}{i} = \frac{35a}{\frac{a}{\sqrt{12}}} \approx 121.24 .$$

In the second case, the cross-section has a width $b = a$ and a height $h = 2a$, yielding

$$\begin{cases} i^2 = \frac{I}{\Omega} = \frac{a \times (2a)^3}{12} \times \frac{1}{2a^2} = \frac{a^2}{3} \\ l_e = 2l = 2 \times 50a = 100a \end{cases} \Rightarrow \lambda = \frac{l_e}{i} = \frac{100a}{\frac{a}{\sqrt{3}}} \approx 173.21 .$$

We conclude that the second possibility corresponds to the actual buckling mode. Since the axial force in the column is $N = 31.25pa$, the critical load takes the value

$$\begin{aligned} \lambda = \frac{100a}{\frac{a}{\sqrt{3}}} &\Rightarrow \sigma_{cr} = \frac{\pi^2 E}{\lambda^2} = \frac{\pi^2 E}{30000} ; \\ \sigma = \sigma_{cr} &\Rightarrow \frac{N}{\Omega} = \frac{31.25 p_{cr} a}{2a^2} = \frac{\pi^2 E}{30000} \Rightarrow p_{cr} = \frac{\pi^2 E a}{468750} . \end{aligned}$$

XI.9 Consider a bar with two built-in ends, with length l and a cross-section with area Ω and moment of inertia I , made of a material with an elasticity modulus E and a thermal expansion coefficient α . Determine the value of a uniform temperature increase Δt which causes a transversal deflection of the bar.

Resolution

The uniform temperature increase Δt introduces into the bar a compressive axial force with the value (see example VI.3)

$$N = E\Omega\alpha\Delta t .$$

The transversal deflection will take place when this value reaches the critical load of the bar. Since the effective length of a bar with two built-in ends is $\frac{l}{2}$, we have

$$N = N_{cr} \Rightarrow E\Omega\alpha\Delta t = \frac{\pi^2 EI}{\left(\frac{l}{2}\right)^2} \Rightarrow \Delta t = \frac{4\pi^2 I}{l^2 \Omega \alpha} = \frac{4\pi^2}{\left(\frac{l}{i}\right)^2 \alpha} .$$

Considering, for example, a steel bar ($\alpha = 1.2 \times 10^{-5}/^\circ C$) with a ratio $\frac{l}{i} = 300$ (slenderness ratio $\lambda = \frac{l}{2i} = 150$), a temperature increase $\Delta t = 36.55^\circ C$, is enough to cause the transversal deflection.

XI.10 The plane structure represented in Fig. XI.10-a is stabilized by means of the cables with cross-section area Ω represented in the Figure. The columns and the cables are made of the same material which has an elasticity modulus E . The cables are not connected to each other in their intersection. The cross-section of the columns has the moment of inertia $I = \frac{\Omega l^2}{125}$.

Determine the critical load of this structure and indicate if it may be able to withstand a higher load than the critical one.

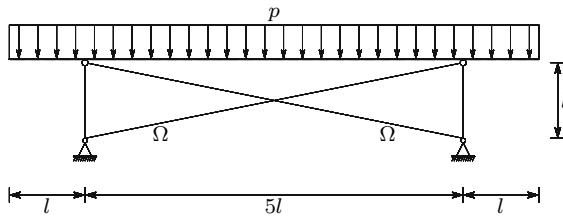


Fig. XI.10-a

Resolution

This structure may become unstable, either by buckling of the columns, or by a horizontal translation of the beam with elongation of one of the cables. The first situation will occur if load p reaches the value corresponding to the buckling axial force of the columns. In this case, we have

$$N_p = \frac{7pl}{2} = \frac{\pi^2 EI}{l^2} \Rightarrow \frac{7pl}{2} = \frac{\pi^2 E \frac{\Omega l^2}{125}}{l^2} \Rightarrow p = p_1 = \frac{2\pi^2 E \Omega}{875 l} \approx 0.0225591 \frac{E \Omega}{l} .$$

In the buckling mode corresponding to the horizontal translation of the beam, the motion represented in Fig. XI.10-b takes place.

The compressive axial forces in the columns, N_p , have a destabilizing horizontal component, since it acts in the direction of the perturbation θl , while the axial force, N_c , in the elongated cable has a stabilizing effect, since it opposes the perturbation. The elongation of this cable and the corresponding axial force take the values

$$\Delta l = \theta l \cos \left(\arctan \frac{l}{5l} \right) \Rightarrow N_c = \Delta l \frac{E\Omega}{\sqrt{l^2 + (5l)^2}} = \frac{\cos \left(\arctan \frac{1}{5} \right)}{\sqrt{26}} E\Omega \theta .$$

In the critical situation the horizontal components of the compressive axial forces in the columns equilibrate the horizontal component of the tensile axial force in the cable. This condition may be used to get the critical load corresponding to this buckling mode, yielding

$$\begin{aligned} 2N_p \theta &= N_c \cos \left(\arctan \frac{1}{5} \right) \Rightarrow 2 \frac{7pl}{2} \theta = \frac{\cos^2 \left(\arctan \frac{1}{5} \right)}{\sqrt{26}} E\Omega \theta \\ \Rightarrow p &= p_2 = \frac{\cos^2 \left(\arctan \frac{1}{5} \right)}{7\sqrt{26}} \frac{E\Omega}{l} \approx 0.0269390 \frac{E\Omega}{l} . \end{aligned}$$

Since $p_1 < p_2$, we conclude that the critical load of the structure takes the value $p = \frac{2\pi^2}{875} \frac{E\Omega}{l}$. Furthermore, we may conclude that this structure may be able to withstand a value of p greater than this (but smaller than p_2), since a compressed bar has a stable post-critical behaviour. If the second mode of instability were to take place ($P_{cr} = p_2$), the post-critical behaviour would be of the same type as the examples in Figs. 155-d and 158-b, i.e., it would be unstable.

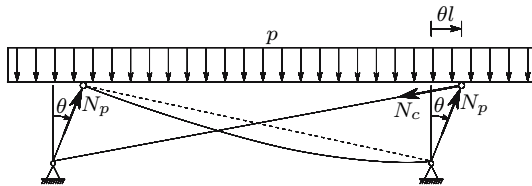


Fig. XI.10-b

XI.11 Considering as rigid the segment AB of the column represented in Fig. XI.11-a, determine its effective length.

Resolution

The problem may be solved by means of a procedure which is similar to that used to compute the effective length of the column represented in Fig. 166-d.

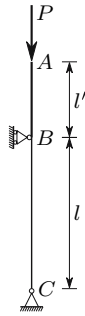


Fig. XI.11-a

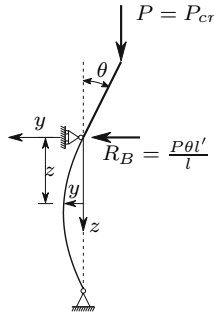


Fig. XI.11-b

Considering the deformed configuration defined by the infinitesimal angle θ (Fig. XI.11-b), the reaction force in support B may be computed by means of the condition of a vanishing bending moment in hinge C , yielding

$$R_B \times l = P \times \theta l' \Rightarrow R_B = \frac{P\theta l'}{l} .$$

The differential equation defining the interaction between bending moments and bending deformations may be found by expressing the bending moment in the cross-section at the distance z from support B (M is positive when it induces a positive curvature in reference system yz) as a function of the curvature, yielding

$$\begin{cases} M(z) = -P \times (y + \theta l') + \frac{P\theta l'}{l} \times z \\ \frac{M}{EI} = \frac{d^2 y}{dz^2} \end{cases} \Rightarrow \frac{d^2 y}{dz^2} + \frac{P}{EI} y = \frac{P}{EI} \theta l' \left(\frac{z}{l} - 1 \right) .$$

This equation admits the particular integral $y = \theta l' \left(\frac{z}{l} - 1 \right)$. Thus, the general solution takes the form

$$y = C_1 \cos(kz) + C_2 \sin(kz) + \theta l' \left(\frac{z}{l} - 1 \right) \quad \text{with} \quad k^2 = \frac{P}{EI} .$$

Differentiating with respect to z , we get the slope of the deflection line which is given by the expression

$$\frac{dy}{dz} = -kC_1 \sin(kz) + kC_2 \cos(kz) + \theta \frac{l'}{l} .$$

By means of the compatibility condition in support B , C_1 and C_2 may be expressed as functions of θ , yielding

$$z = 0 \Rightarrow \begin{cases} y = 0 \Rightarrow C_1 = \theta l' \\ \frac{dy}{dz} = \theta \Rightarrow kC_2 + \theta \frac{l'}{l} = \theta \Rightarrow C_2 = \theta \frac{l-l'}{kl} . \end{cases}$$

Substituting these values in the general solution, we get

$$y = \theta \left[l' \cos(kz) + \frac{l-l'}{kl} \sin(kz) + l' \left(\frac{z}{l} - 1 \right) \right].$$

The condition of a vanishing deflection in point C leads to the conclusion

$$z = l \Rightarrow y = 0 \Rightarrow \theta = 0 \quad \vee \quad l' \cos(kl) + \frac{l-l'}{kl} \sin(kl) = 0.$$

The first alternative ($\theta = 0$) corresponds to the undeformed configuration. The second possibility corresponds to the equilibrium in a slightly deformed configuration, allowing the computation of the critical load. This equation takes especially simple forms in two cases. In the first, $l' = 0$, we get Euler's solution for a pin-ended bar, $\sin(kl) = 0$, as expected. In the second, $l' = l$, we have

$$l' \cos(kl) = 0 \Rightarrow kl = \frac{\pi}{2} \Rightarrow \frac{P}{EI} l^2 = \left(\frac{\pi}{2} \right)^2 \Rightarrow P = \frac{\pi^2 EI}{l_e^2} \quad \text{with } l_e = 2l.$$

In the general case the value of kl must be found by numerical means, since it is a transcendental equation. Determining the least value of kl which satisfies the condition

$$\frac{l'}{l} \cos(kl) + \left(1 - \frac{l'}{l} \right) \frac{\sin(kl)}{kl} = 0,$$

the effective length is given by the expression

$$(kl)^2 = \frac{Pl^2}{EI} \Rightarrow P = \frac{\pi^2 EI}{l_e^2} \quad \text{with } l_e = \frac{\pi}{kl} l.$$

The following Table gives the results obtained for some given values of the ratio $\frac{l'}{l}$.

$\frac{l'}{l}$	0	0.1	0.5	1	2	4
kl	π	2.836	2.029	1.571	1.166	0.845
l_e	l	1.108l	1.549l	2l	2.695l	3.719l

XI.12 Determine the critical load of the column represented in Fig. XI.12-a (do not consider the possibility of the buckling of bar AB alone).

Resolution

In the deformed configuration defined by the infinitesimal displacement Δ in hinge B (Fig. XI.12-b) the forces acting on the upper end of bar BC are those represented in Fig. XI.12-c.

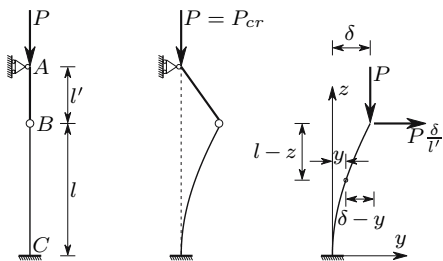


Fig. XI.12-a Fig. XI.12-b Fig. XI.12-c

The differential equation of this problem is

$$\begin{cases} M(z) = P(\delta - y) + P\frac{\delta}{l'}(l - z) \\ \frac{M}{EI} = \frac{d^2y}{dz^2} \end{cases} \Rightarrow \frac{d^2y}{dz^2} + \frac{P}{EI}y = \frac{P}{EI}\delta \left(1 + \frac{l-z}{l'}\right).$$

This equation admits the particular integral $y = \delta \left(1 + \frac{l-z}{l'}\right)$. Thus, the general solution is

$$y = C_1 \cos(kz) + C_2 \sin(kz) + \delta \left(1 + \frac{l-z}{l'}\right) \quad \text{with} \quad k^2 = \frac{P}{EI}.$$

Derivation with respect to z yields the slope of the deflection line

$$\frac{dy}{dz} = -kC_1 \sin(kz) + kC_2 \cos(kz) - \frac{\delta}{l'}.$$

The compatibility conditions in support C enable the integration constants C_1 and C_2 to be expressed as functions of δ , yielding

$$z = 0 \Rightarrow \begin{cases} y = 0 \Rightarrow C_1 + \delta \left(1 + \frac{l}{l'}\right) = 0 \Rightarrow C_1 = -\delta \frac{l+l'}{l'} \\ \frac{dy}{dz} = 0 \Rightarrow kC_2 - \frac{\delta}{l'} = 0 \Rightarrow C_2 = \frac{\delta}{kl'}. \end{cases}$$

Substituting these values in the general solution, we get

$$y = \delta \left[\frac{\sin(kz)}{kl'} - \frac{l+l'}{l'} \cos(kz) + 1 + \frac{l-z}{l'} \right].$$

In point B this equation must yield the value δ . Thus, we have

$$\begin{aligned} z = l \Rightarrow y = \delta &\Rightarrow \delta \left[\frac{\sin(kl)}{kl'} - \frac{l+l'}{l'} \cos(kl) + 1 \right] = \delta \\ \Rightarrow \delta \left[\frac{\sin(kl)}{kl'} - \frac{l+l'}{l'} \cos(kl) \right] &= 0 \Rightarrow \delta = 0 \vee \frac{\sin(kl)}{kl'} - \frac{l+l'}{l'} \cos(kl) = 0. \end{aligned}$$

Like example XI.11 the first possibility ($\Delta = 0$) corresponds to an undeformed configuration, so that it cannot be used to compute the critical load.

The second alternative corresponds to the equilibrium in a slightly deformed configuration. Thus, the critical load may be obtained from the condition

$$\frac{\sin(kl)}{kl'} = \frac{l+l'}{l'} \cos(kl) \Rightarrow \left(1 + \frac{l'}{l}\right) kl = \tan(kl).$$

Note that for $l' = 0$ we get to the same problem as that represented in Fig. 166-d, $kl = \tan(kl)$, $l_e = 0.7l$. With $l' = \infty$ the example in Fig. 166-a is obtained ($kl = \frac{\pi}{2}$), $l_e = 2l$, since the pin-ended bar AB remains vertical for any value of Δ . For other values of l' , we conclude that the higher the value of l' , the higher is the critical load, as indicated in the following table.

$\frac{l'}{l}$	0	0.1	0.2	0.5	1	10	∞
kl	4.493	0.5175	0.6955	0.9674	1.166	1.511	$\frac{\pi}{2}$
l_e	$0.6992l$	$6.071l$	$4.517l$	$3.247l$	$2.695l$	$2.080l$	$2l$

XI.13 Find the critical load of the column depicted in Fig. XI.13-a.

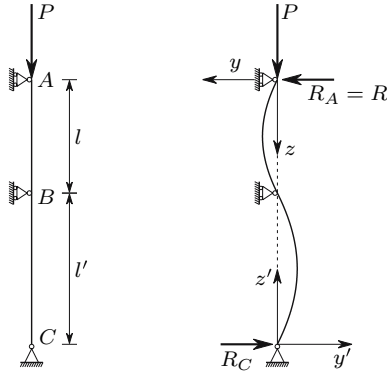


Fig. XI.13-a Fig. XI.13-b

Resolution

Considering the deformed configuration and the two reference systems represented in Fig. XI.13-b, the differential equation corresponding to segment AB takes the form ($M(z) = -Py + R_A z$)

$$\frac{d^2y}{dz^2} + \frac{P}{EI}y = \frac{R_A}{EI}z.$$

This equation admits the particular integral $y = \frac{R_A}{P}z$. Thus, its general solution is given by the expression

$$y = C_1 \cos(kz) + C_2 \sin(kz) + \frac{R_A}{P} z \quad \text{with} \quad k^2 = \frac{P}{EI}.$$

Using the conditions of zero deflection in supports A and B , the integration constants may be related to the reaction force R_A , yielding

$$\begin{aligned} z = 0 &\Rightarrow y = 0 \Rightarrow C_1 = 0 \\ z = l &\Rightarrow y = 0 \Rightarrow C_2 \sin(kl) + \frac{R_A}{P} l = 0 \Rightarrow C_2 = -\frac{R_A}{P} \frac{l}{\sin(kl)}. \end{aligned}$$

Substituting these values in the general solution and derivating, we get the rotation as a function of coordinate z

$$y = \frac{R_A}{P} \left[z - \frac{l}{\sin(kl)} \sin(kz) \right] \Rightarrow \frac{dy}{dz} = \frac{R_A}{P} \left[1 - \frac{kl}{\sin(kl)} \cos(kz) \right].$$

In cross-section B this rotation takes the value

$$\left(\frac{dy}{dz} \right)_{z=l} = \frac{R_A}{P} \left[1 - \frac{kl}{\tan(kl)} \right] = \frac{R}{P} \left[1 - \frac{kl}{\tan(kl)} \right].$$

Note that by equating this rotation to zero, we get the problem represented in Fig. 166-d.

This rotation may also be obtained from the deformation of the column segment BC . The procedure is exactly the same as in segment AB , so we may simply substitute y by y' , z by z' , l by l' and R_A by R_C . Using the moment balance condition with respect to point B , this reaction force may be related to R , yielding $R_C = -R \frac{l}{l'}$. The minus sign is a consequence of the positive directions adopted for the reaction forces, whose objective was that of having analogous equations in segments AB and BC . The rotation of cross-section B is then also given by the expression

$$\left(\frac{dy'}{dz'} \right)_{z'=l'} = \frac{R_C}{P} \left[1 - \frac{kl'}{\tan(kl')} \right] = -\frac{R}{P} \frac{l}{l'} \left[1 - \frac{kl'}{\tan(kl')} \right].$$

The condition of continuity in point B leads to the condition

$$\left(\frac{dy}{dz} \right)_{z=l} = \left(\frac{dy'}{dz'} \right)_{z'=l'} \Rightarrow \frac{R}{P} \left[1 - \frac{kl}{\tan(kl)} \right] = -\frac{R}{P} \frac{l}{l'} \left[1 - \frac{kl'}{\tan(kl')} \right].$$

If the reaction force R is not zero, this equation is equivalent to

$$1 - \frac{kl}{\tan(kl)} = -\frac{l}{l'} + \frac{kl}{\tan(kl \frac{l'}{l})} \Rightarrow \frac{kl}{\tan(kl)} + \frac{kl}{\tan(\frac{kl}{\alpha})} = 1 + \alpha \quad \text{with} \quad \alpha = \frac{l}{l'}.$$

The smallest of the roots of this transcendental equation is the value of kl which corresponds to the critical load. However, it must be noted that this expression does not completely define the problem. In fact, if we have $l = l'$, we will have $R = 0$, since the deformed configuration is antisymmetric, which

means that the bending moment vanishes in cross-section B . This corresponds to the second buckling mode in Fig. 165 ($n = 2$). In the case of $l = l'$ the smallest of the roots of this equation is $kl = 4.4934$. However, the equilibrium in a slightly deformed configuration requires that integration constant C_2 does not vanish ($C_2 \neq 0$), since $R_A = 0$. This implies that $\sin(kl) = 0$, i.e., $kl = n\pi$. When $l \neq l'$, R cannot vanish, since this would mean that two pin-ended columns with different lengths would have the same critical load. In the following Table the smallest roots are given for some values of α .

α	0.01	0.05	0.1	0.5	0.99	1.01	2	5	10	∞
kl	0.04479	0.2211	0.4352	1.928	3.126	3.157	3.857	4.223	4.352	4.493

XI.14 Determine the maximum bending moment in the column represented in Fig. XI.14.

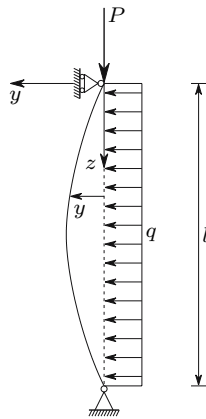


Fig. XI.14

Resolution

Considering as positive the bending moments which correspond to a positive curvature in reference system yz , the bending moment in the cross-section defined by coordinate z is given by the expression

$$M = -Py - \frac{ql}{2}z + \frac{q}{2}z^2.$$

Since the moment-curvature relation in the same reference system may also be expressed by $M = EI \frac{d^2y}{dz^2}$, the differential equation which defines the deformation of the column takes the form

$$\frac{d^2y}{dz^2} + \frac{P}{EI}y = \frac{q}{EI}y \left(-\frac{l}{2}z + \frac{z^2}{2} \right).$$

Since this equation admits the particular integral

$$y = \frac{q}{P} \left(\frac{z^2}{2} - \frac{l}{2}z \right) - \frac{EI}{P^2}q,$$

the general solution is

$$y = C_1 \sin(kz) + C_2 \cos(kz) + \frac{q}{P} \left(\frac{z^2}{2} - \frac{l}{2}z \right) - \frac{q}{Pk^2} \quad \text{with} \quad k^2 = \frac{P}{EI}.$$

The integration constants may be found by means of the support conditions, yielding

$$\begin{aligned} z = 0 &\Rightarrow y = 0 \Rightarrow C_2 = \frac{q}{Pk^2} \\ z = l &\Rightarrow y = 0 \Rightarrow C_1 \sin(kl) + \frac{q}{Pk^2} \cos(kl) - \frac{q}{Pk^2} = 0 \\ &\Rightarrow C_1 = \frac{q}{Pk^2} \frac{1 - \cos(kl)}{\sin(kl)}. \end{aligned}$$

Substituting these quantities in the general solution, we get the displacement y in the cross-section defined by coordinate z

$$y = \frac{q}{Pk^2} \left[\frac{1 - \cos(kl)}{\sin(kl)} \sin(kz) + \cos(kz) - 1 \right] + \frac{q}{P} \left(\frac{z^2}{2} - \frac{l}{2}z \right).$$

This function reaches a maximum for $z = \frac{l}{2}$, as may be concluded by symmetry considerations, and is confirmed by differentiation

$$\begin{aligned} \frac{dy}{dz} &= \frac{q}{Pk^2} \left[\frac{1 - \cos(kl)}{\sin(kl)} k \cos(kz) - k \sin(kz) \right] + \frac{q}{P} \left(z - \frac{l}{2} \right); \\ z = \frac{l}{2} &\Rightarrow \frac{dy}{dz} = \frac{q}{Pk} \left[\frac{1 - \cos(kl)}{\sin(kl)} \cos\left(k\frac{l}{2}\right) - \sin\left(k\frac{l}{2}\right) \right] \\ &= \frac{q}{Pk} \left[\frac{2 \sin^2\left(\frac{kl}{2}\right)}{2 \sin\left(\frac{kl}{2}\right) \cos\left(\frac{kl}{2}\right)} \cos\left(k\frac{l}{2}\right) - \sin\left(k\frac{l}{2}\right) \right] = 0. \end{aligned}$$

Thus, the maximum displacement occurs for $z = \frac{l}{2}$ and takes the value

$$z = \frac{l}{2} \Rightarrow y = y_{\max} = \frac{q}{Pk^2} \left[\frac{\sin^2\left(\frac{kl}{2}\right)}{\cos\left(\frac{kl}{2}\right)} + \cos\left(\frac{kl}{2}\right) - 1 \right] - \frac{q}{P} \frac{l^2}{8},$$

since $\frac{1 - \cos(kl)}{\sin(kl)} = \frac{\sin\left(\frac{kl}{2}\right)}{\cos\left(\frac{kl}{2}\right)}$. The maximum value of the bending moment is then

$$M_{\max} = Py_{\max} + \frac{ql^2}{8} = \frac{q}{k^2} \left[\frac{\sin^2\left(\frac{kl}{2}\right)}{\cos\left(\frac{kl}{2}\right)} + \cos\left(\frac{kl}{2}\right) - 1 \right] = \frac{q}{k^2} \frac{1 - \cos\left(\frac{kl}{2}\right)}{\cos\left(\frac{kl}{2}\right)} .$$

Instability by divergence takes place for $kl = \pi$ ($M_{\max} = \infty$), as expected, since the transversal load q does not influence the value of the critical load. If we consider $k = 0$, the expression of M_{\max} becomes indeterminate. This problem may be solved by means of L'Hôpital's rule, yielding, as expected, the expression of the maximum bending moment in a simply supported beam with span l under the action of a uniformly distributed load q ,

$$\lim_{k \rightarrow 0} M_{\max} = \lim_{k \rightarrow 0} q \frac{1 - \cos\left(\frac{kl}{2}\right)}{k^2 \cos\left(\frac{kl}{2}\right)} = \frac{ql^2}{8} .$$

XI.15 Figure XI.15 represents the cross-section of a bar which supports an axial compressive force P . Determine:

- the value of P which causes torsional buckling of the bar;
- the maximum slenderness ratio, so that torsional buckling occurs before bending buckling, considering $d = 20e$ and $\nu = 0.3$.

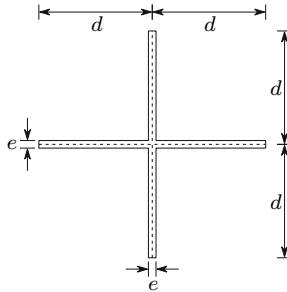


Fig. XI.15

Resolution

- The critical load for torsional buckling may be found by means of the equilibrium conditions of the forces applied to a bar segment with unit length in the deformed configuration defined by the infinitesimal angle θ (Fig. XI.15-a). The vector representing the force per surface unit acting on each point of the upper cross-section may be decomposed into two components: one parallel to the fibres (Fig. XI.15-b) and other in the plane defined by the wall's centre lines of the cross-section (Fig. XI.15-c). The first one does not cause torsion, since it is balanced by the normal stresses acting on facets that are perpendicular to the fibres of the deformed bar (it may be accepted that the shearing stresses perpendicular to the wall centre line vanish in all these facets, since this cross-section has thin walls).

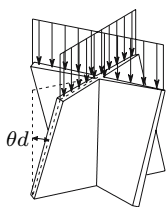


Fig. XI.15-a

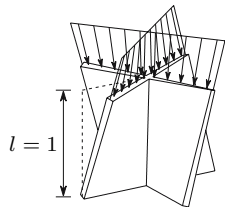


Fig. XI.15-b

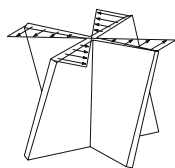


Fig. XI.15-c

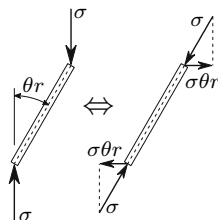


Fig. XI.15-d

The second component, on the other side, introduces a twisting moment in the same direction as the rotation θ .

The rotation of the fibres caused by the torsional deformation θ is θr , where r is the distance of the fibre to the bar's axis ($0 \leq r \leq d$). Thus, the second component takes the value $\sigma \theta r$ (Fig. XI.15-d). The total twisting moment needed to keep the torsional deformation defined by θ is then (GJ is the torsional stiffness, as defined by (246))

$$T = GJ\theta - 4 \int_0^d r\sigma\theta r e dr = G\theta 4 \frac{1}{3} d e^3 - 4\theta\sigma e \frac{d^3}{3} = \frac{4}{3}\theta d e (G e^2 - \sigma d^2) .$$

In the critical phase this twisting moment vanishes. Thus, the critical load for torsional buckling takes the value

$$T = 0 \Rightarrow \sigma = \sigma_{cr}^t = G \left(\frac{e}{d} \right)^2 \Rightarrow P_{cr}^t = \Omega \sigma_{cr}^t = 4 d e \sigma_{cr}^t = 4 G \frac{e^3}{d} .$$

(b) For $d = 20e$ the critical stress for torsional buckling takes the value

$$d = 20e \Rightarrow \sigma_{cr}^t = \frac{G}{400} .$$

In the case of bending buckling the critical stress takes the value

$$\begin{aligned} I &= \frac{2de^3}{12} + \frac{e(2d)^3}{12} = \frac{de}{6} (e^2 + 4d^2) \\ \Rightarrow i^2 &= \frac{I}{\Omega} = \frac{\frac{de}{6} (e^2 + 4d^2)}{4de} = \frac{1}{24} (e^2 + 4d^2) = \frac{1601}{24} e^2 \\ \Rightarrow \sigma_{cr}^f &= \frac{\pi^2 E i^2}{l^2} = \frac{\pi^2 E}{l^2} \frac{1601}{24} e^2 . \end{aligned}$$

Torsional buckling will take place if the corresponding critical stress is smaller than the value corresponding to bending buckling, that is, if

$$\begin{aligned} \sigma_{cr}^f > \sigma_{cr}^t &\Rightarrow \frac{\pi^2 E}{l^2} \frac{1601}{24} e^2 > \frac{E}{2(1+\nu)} \frac{1}{400} \\ &\Rightarrow l^2 < \pi^2 e^2 \frac{1601}{24} \times 400 \times 2(1+\nu) . \end{aligned}$$

The given value for the Poisson coefficient ($\nu = 0.3$) yields

$$\nu = 0.3 \Rightarrow l < 827.48e = 41.37d .$$

The slenderness ratio corresponding to this length is

$$\lambda = \frac{l}{i} = \frac{827.48}{\sqrt{\frac{1601}{24}}} = 101.31 .$$

XI.16 The stress-strain relation for aluminium may be defined by means of the so-called Ramberg-Osgood equation which takes the form (Fig. XI.16)

$$\varepsilon = \frac{\sigma}{E} + 0.002 \left(\frac{\sigma}{\sigma_{0.2}} \right)^n \quad \text{with} \quad \begin{cases} E = 70\,000 \text{ MPa} \\ \sigma_{0.2} = 277 \text{ MPa} \\ n = 18.55 . \end{cases}$$

- (a) Verify the stability of a pin-ended bar with length $l = 3\text{m}$ and hollow square cross-section with outside side-length of 15cm and wall-thickness of 2.5mm , under a compressive axial force $N = 250\text{kN}$.
- (b) Determine the critical load.

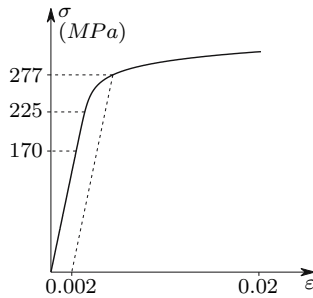


Fig. XI.16

Resolution

- (a) The area and the moment of inertia of the bar's cross-section are, respectively

$$\Omega = 0.15^2 - 0.145^2 = 1.475 \times 10^{-3} \text{m}^2$$

$$I = \frac{0.15^4 - 0.145^4}{12} = 5.350 \times 10^{-6} \text{m}^4 .$$

Since the constitutive law is not linear, it is necessary to compute the tangent modulus of elasticity corresponding to the stress acting on the

bar. Since the strain is defined as a function of the stress, the computation may be performed by the expressions

$$\sigma = \frac{N}{\Omega} \longrightarrow E_t = \frac{d\sigma}{d\varepsilon} = \left(\frac{d\varepsilon}{d\sigma} \right)^{-1} = \left[\frac{1}{E} + 0.002 n \left(\frac{\sigma}{\sigma_{0.2}} \right)^{n-1} \frac{1}{\sigma_{0.2}} \right]^{-1} .$$

Substituting the parameters contained in these expressions by the given values, we get

$$\sigma = 169.492 \text{ MPa} \longrightarrow E_t = 69.882 \text{ GPa} .$$

If this value were to remain constant, the critical load of the bar would be

$$P_{cr} = \frac{\pi^2 E_t I}{l^2} = 409988 \text{ N} .$$

This value exceeds the applied axial load, $N = 250 \text{ kN}$. This is not the actual value of the critical load, since the tangent elasticity modulus corresponding to this axial force (409988 N) is smaller than the value used which corresponds to 250 kN . However, the fact that this value is larger than the applied axial force indicates that the actual value of the critical load lies between these two values, which means that the bar is stable.

- (b) The critical load may be obtained by means of successive approximations, or by more sophisticated numerical methods for solving non-linear equations. Convergence is attained, when the critical load computed by means of the procedure used in answer to question a) is equal to the value of the axial force used to compute the tangent modulus of elasticity.

In the present case the solution has been computed by increasing the value of N by 5% of the difference between N and the value of P_{cr} corresponding to $E_t(N)$. Convergence has been reached after 60 iterations, yielding the results

$$P_{cr} = 331483 \text{ N}, \quad \sigma_{cr} = 224.734 \text{ MPa} \quad \text{and} \quad E_t = 56.501 \text{ GPa} .$$

It must be noted that the simple successive substitution (substitution of N by the value of P_{cr} obtained from it) does not converge in this case.

Remark: Although in the diagram presented in Fig. XI.16 (which exactly represents the Ramberg-Osgood equation given) the difference between the elasticity moduli corresponding to the given ($\sigma \approx 170 \text{ MPa}$) and critical ($\sigma \approx 225 \text{ MPa}$) stresses is too small to be observed, the actual critical load is substantially smaller than that corresponding to the first value. This example illustrates the error introduced when Euler's formula is used above the proportionally limit without considering the reduction of the elasticity modulus.

XI.17 Compare the values obtained for the maximum load under eccentric compression using the exact solution (261) and the interaction formula. Consider a grade *S 355* steel and the values 0.001, 0.25 and 1 (Fig. 170) for the eccentricity ratio α .

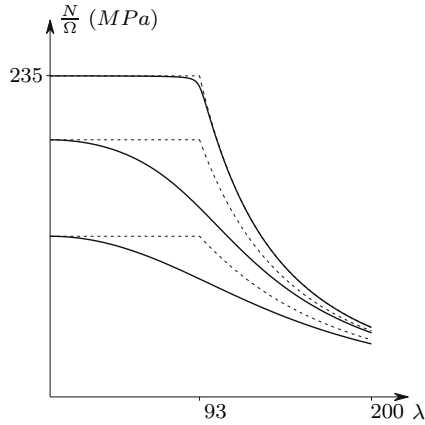


Fig. XI.17

Resolution

In the case of plane composed bending caused by an eccentric compression the interaction formula may be given the form

$$\left\{ \begin{array}{l} M = Pe \\ I = \Omega i^2 \\ \frac{P}{\Omega \varphi} + \frac{M}{I} \leq \sigma_{\text{all}} \end{array} \right. \Rightarrow \frac{P}{\Omega} \left(\frac{1}{\varphi} + \frac{ve}{i^2} \right) \leq \sigma_{\text{all}} \Rightarrow \frac{P}{\Omega} \left(\frac{1}{\varphi} + \alpha \right) \leq \sigma_{\text{all}} .$$

In order to facilitate the comparison, no safety coefficients are considered and the allowable stress σ_{all} is assumed to be under the proportionality limit. Under these conditions φ is given by Euler's formula for values of λ higher than

$$\frac{\pi^2 E}{\lambda^2} = \sigma_{\text{all}} \Rightarrow \lambda = \pi \sqrt{\frac{E}{\sigma_{\text{all}}}} = \pi \sqrt{\frac{206000}{235}} = 93.0 .$$

Thus, we get the following expressions for parameter φ

$$\lambda \leq 93 \Rightarrow \varphi = 1 ; \quad \lambda > 93 \Rightarrow \varphi = \frac{\pi^2 E}{\lambda^2 \sigma_{\text{all}}} .$$

The maximum load that may be applied, so that the stress does not exceed the value σ_{all} , may thus be defined by the expression

$$\frac{P}{\Omega} = \frac{\sigma_{\text{all}}}{\frac{1}{\varphi} + \alpha} .$$

The dashed lines in Fig. XI.17 represent the curves which define $\frac{P}{\Omega}$ as a function of λ for the given values of α . The solid lines represent the exact curves

which are those depicted in Fig. 170. We find that for a small eccentricity ($\alpha = 0.001$) the curves practically coincide, since in this case the axial force is virtually centred. For the other two values of α , considerable differences are observed. Furthermore, the error has an adverse effect on structural safety, since the loading capacity is overestimated. However, this error is covered by the larger additional safety coefficients used in the safety evaluation of long members. Furthermore, the error attains a maximum in the region where Euler's curve is usually substituted by smoother approximation curves (Fig. 167), which reduces the peak corresponding to $\lambda = 93$.

XI.18 Determine the eccentricities corresponding to the values of parameter α considered in Fig. 170 in a rectangular cross-section with width b .

XI.19 In the structure represented in Fig. XI.19 the spring has a stiffness E and bars AB and AC may be considered as rigid. Support C prevents displacement in the direction of bar AC . Determine the critical load of the structure.

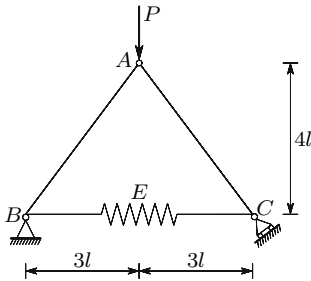


Fig. XI.19

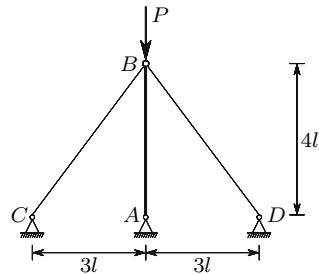


Fig. XI.20

XI.21 Determine whether the spring is necessary to stabilize the plane structure represented in Fig. XI.21. If it is, determine the critical load of the structure.

XI.22 Using the results of example XI.13, determine the critical load of the structure represented in Fig. XI.22.

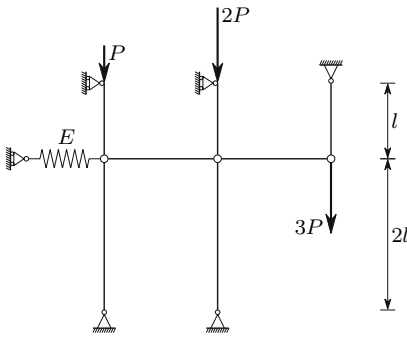


Fig. XI.21

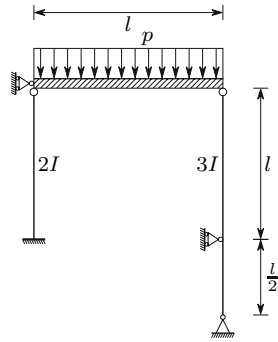


Fig. XI.22

XI.23 The beam represented in Fig. XI.23 has a bending stiffness EI . Taking the interaction between deformation and internal forces into consideration determine the maximum bending moment.

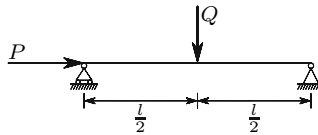


Fig. XI.23

XI.6 Stability Analysis by the Displacement Method

XI.6.a Introduction

In Sects. XI.2 to XI.5 problems of stability have been analysed whose degrees of kinematic indeterminacy are one (introductory examples in Sect. XI.2) or infinite (Euler's theory furnishes an infinite number of buckling shapes). However, in the modern computational analysis of structures, a finite number of degrees of freedom is always considered, either in naturally discrete structures, such as framed structures, or in finite-element discretizations of two- or three-dimensional structures.

In this section we will introduce the global stability analysis of framed structures by means of the displacement method. However, this analysis does not belong to the traditional field of Strength of Materials, since it is based on the matrix formulation used in the systematization of the displacement method, which is usually taught after the Strength of Materials has been studied, in the disciplines of Structural Analysis. This is why this analysis is explained as an appendix to Chap. XI.

XI.6.b Simple Examples

As a first example of a naturally discrete structure with a degree of kinematic indeterminacy superior to one, we shall analyse the stability behaviour of the column represented in Fig. 172-a.

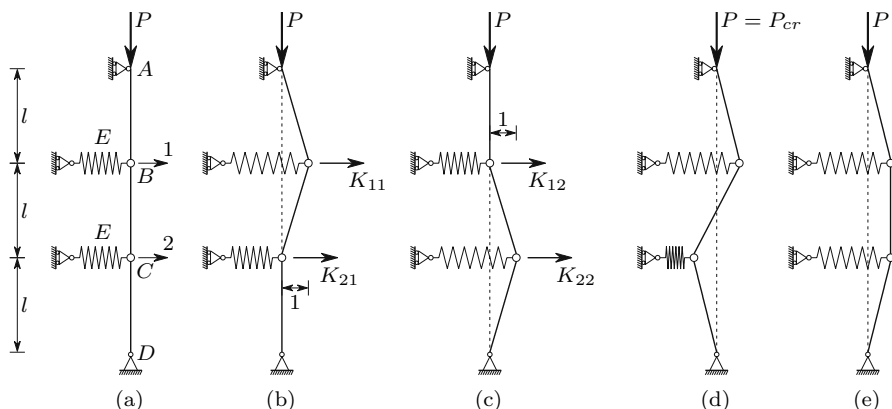


Fig. 172. Stability analysis of a structure with degree two of kinematic indeterminacy

If the vertical bars are assumed to be axially non-deformable, this structure has a degree two of kinematic indeterminacy, since, once the horizontal displacements of points B and C are known (coordinates 1 and 2 in Fig. 172-a), the deformed configuration of the structure is completely defined. Assuming that there are no imperfections, no deformations will take place as long as the structure is stable, since no forces are needed in the deformable elements to balance the external force P .

Let us consider now that two forces, F_1 and F_2 , are applied in coordinates 1 and 2, respectively. These forces will cause displacements D_1 and D_2 . Conversely, we may state that, in order to get the deformed configuration defined by displacements D_1 and D_2 , corresponding forces F_1 and F_2 must be applied in coordinates 1 and 2. The force-displacement relations may be represented by the expression

$$\begin{cases} F_1 = F_1(D_1, D_2) \\ F_2 = F_2(D_1, D_2) \end{cases} .$$

If the displacements D_1 and D_2 are infinitesimal, the corresponding forces are given by the expressions

$$\begin{cases} dF_1 = \frac{\partial F_1}{\partial D_1} dD_1 + \frac{\partial F_1}{\partial D_2} dD_2 \\ dF_2 = \frac{\partial F_2}{\partial D_1} dD_1 + \frac{\partial F_2}{\partial D_2} dD_2 \end{cases} . \tag{262}$$

Using a matrix formulation, the expression may be written as

$$\begin{Bmatrix} dF_1 \\ dF_2 \end{Bmatrix} = \underbrace{\begin{bmatrix} \frac{\partial F_1}{\partial D_1} = K_{11} & \frac{\partial F_1}{\partial D_2} = K_{12} \\ \frac{\partial F_2}{\partial D_1} = K_{21} & \frac{\partial F_2}{\partial D_2} = K_{22} \end{bmatrix}}_{[K]} \begin{Bmatrix} dD_1 \\ dD_2 \end{Bmatrix}.$$

Matrix $[K]$ is the so-called *stiffness matrix* of the structure. It may be shown that this matrix is symmetrical (see Sect. XII.4).

In the critical situation the equilibrium state is neutral, that is, it is not disturbed when the equilibrium configuration suffers an infinitesimal perturbation, which may be defined by the displacements dD_1 and dD_2 . This means that the infinitesimal forces corresponding to these displacements, dF_1 and dF_2 , vanish when force P attains the critical value. This condition may be expressed by the relation

$$\begin{bmatrix} K_{11} & K_{12} \\ K_{21} & K_{22} \end{bmatrix} \begin{Bmatrix} dD_1 \\ dD_2 \end{Bmatrix} = \begin{Bmatrix} 0 \\ 0 \end{Bmatrix}. \quad (263)$$

This system of equations is homogeneous, which means that it only has non-simultaneously vanishing solutions if matrix $[K]$ is singular, i.e., if its determinant is zero. Since this is what happens in the critical phase – a deformed configuration is possible, without forces being applied in the nodal points – the condition $|K| = 0$ may be used to find the critical load of the structure.

As an alternative to the derivation of the force-displacement relations (262), which would require those functions to be found, the elements of the stiffness matrix may be determined directly by means of equilibrium considerations, assuming given values for the displacements dD_1 and dD_2 . Thus, we get from (262)

$$\begin{cases} dD_1 = 1 \\ dD_2 = 0 \end{cases} \Rightarrow \begin{cases} dF_1 = \frac{\partial F_1}{\partial D_1} = K_{11} \\ dF_2 = \frac{\partial F_2}{\partial D_1} = K_{21} \end{cases}. \quad (264)$$

From these expressions we conclude that the stiffness coefficients K_{11} and K_{21} are the forces that must be applied in coordinates 1 and 2, to get the deformed configuration depicted in Fig. 172-b. Since the unit displacement dD_1 is infinitesimal, the axial force in the bars is P and the rotations of bars AB and BC are $\frac{1}{l}$. Therefore, the stiffness coefficient K_{11} is the force needed to induce a unit elongation in the spring and to balance the horizontal components of the axial forces in bars AB and BC . K_{21} is the force required to balance the horizontal component of the axial force in bar BC . Thus, these coefficients take the values

$$K_{11} = E - 2\frac{P}{l} \quad K_{21} = \frac{P}{l}.$$

The two remaining coefficients may be found in a similar way, by considering the deformed configuration represented in Fig. 172-c ($dD_1 = 0$, $dD_2 = 1$). The complete stiffness matrix is then

$$[K] = \begin{bmatrix} E - 2\frac{P}{l} & \frac{P}{l} \\ \frac{P}{l} & E - 2\frac{P}{l} \end{bmatrix} = \underbrace{E \begin{bmatrix} 1 & 0 \\ 0 & 1 \end{bmatrix}}_{\text{material stiffness}} + \underbrace{P \begin{bmatrix} -2\frac{1}{l} & \frac{1}{l} \\ \frac{1}{l} & -2\frac{1}{l} \end{bmatrix}}_{\text{geometrical stiffness}}. \quad (265)$$

The *material stiffness* is the component of the stiffness matrix that depends on the stiffness of the deformable elements of the structure: the stiffness of the springs in this case, the modulus of elasticity and the Poisson's coefficient in the case of materials with linear elastic behavior. The *geometrical stiffness* represents the influence of the geometry change of the structure, when it deforms, that is, the change in the nodal forces which equilibrate the internal forces, caused by the change in the directions of the internal forces as a consequence of the rotations. Thus, the geometrical stiffness depends on the internal forces. Tensile internal forces cause a positive geometrical stiffness, while compressive internal forces lead to a negative geometrical stiffness. Buckling occurs when the negative influence of the geometrical stiffness caused by compressive internal forces compensates the positive influence of the material stiffness and of the geometrical stiffness corresponding to tensile internal forces.

Since the stiffness matrix depends on the forces applied to the structure, when it includes the geometrical stiffness, the critical load may be computed by means of the condition of a vanishing determinant, $|K| = 0$, yielding

$$\begin{vmatrix} E - 2\frac{P}{l} & \frac{P}{l} \\ \frac{P}{l} & E - 2\frac{P}{l} \end{vmatrix} = E^2 - \frac{4E}{l}P + \frac{3}{l^2}P^2 = 0 \Rightarrow P = \frac{El}{3} \quad \vee \quad P = El. \quad (266)$$

Thus, there are two values of the load P which satisfy the condition of neutral equilibrium which must be fulfilled in the transition from stable to unstable equilibrium: the same internal forces balance the external loads both in the undeformed and in a slightly deformed configuration. The critical load corresponds to the smallest of these values, that is, the critical load takes the value $P_{cr} = \frac{El}{3}$.

However, the equilibrium in the slightly deformed configuration does not occur for an arbitrary deformation shape, but only if some relations between the nodal displacements are satisfied. These relations define the so-called *buckling modes*. In Euler's problem the buckling modes have sinusoidal shapes, as seen in Subsect. XI.3.b. The shape corresponding to $P = P_{cr}$ defines the deformation of the structure when buckling takes place. This shape, i.e., the relation between dD_1 and dD_2 may be found by substituting P by P_{cr} in the stiffness matrix and assuming a given value for one of the nodal displacements.

ments.⁷ Thus, if we take $dD_1 = 1$, we get from (265) and (263)

$$\begin{cases} P = P_{cr} = \frac{El}{3} \\ dD_1 = 1 \end{cases} \Rightarrow \begin{bmatrix} \frac{E}{3} & \frac{E}{3} \\ \frac{E}{3} & \frac{E}{3} \end{bmatrix} \begin{cases} 1 \\ dD_2 \end{cases} = \begin{cases} 0 \\ 0 \end{cases}.$$

Any of the two equations of this system yields the value -1 for dD_2 . Therefore, when the load attains the critical value, the equilibrium takes place both in the undeformed configuration and in the slightly deformed configuration represented in Fig. 172-d. This configuration defines the *first buckling mode*. The second mode, corresponding to the second root of (266), may be found in the same way as the first one, i.e., by substituting P by El in the stiffness matrix, yielding the shape represented in Fig. 172-e. Obviously, this configuration is unstable, since it corresponds to a larger load than the critical one. This is demonstrated by the negative values of the diagonal elements of the stiffness matrix, $P = El \Rightarrow K_{11} = K_{22} = -E$ (see Subject. XII.5.c).

As a second example of stability analysis in discrete problems with a degree of kinematic indeterminacy superior to one, we shall analyse the column represented in Fig. 173-a, where the stability is guaranteed by the bending stiffness of the two rotational springs, B and C , which have stiffness G .

The line of reasoning used in the first example is obviously also valid in this case, which means that the elements of the stiffness matrix corresponding to the two represented degrees of freedom, 1 and 2, are the forces that must be applied in these coordinates in order to keep the column in the deformed configurations represented in Figs. 173-b ($dD_1 = 1, dD_2 = 0$) and 173-c ($dD_1 = 0, dD_2 = 1$).

The computation of the stiffness coefficients is a little lengthier than in the first example, since in this case the bars are not under purely axial loading, when dD_1 or dD_2 are different from zero. For the computation of K_{11} and K_{21} by means of equilibrium considerations we may first compute the reaction force R_A (Fig. 173-b), using the expression of the bending moment in spring B as a function of R_A , $M_B = P \times 1 - R_A l = G \frac{l^2}{2}$. Then K_{11} may be found using the expression of the bending moment in spring C . Once R_A and K_{11} are known, K_{21} may be obtained from the condition of zero bending moment in hinge D . The same procedure, applied to the configuration represented in Fig. 173-c, yields the values of K_{12} K_{22} . The stiffness matrix is then given by

$$[K] = \begin{bmatrix} \frac{5G}{l^2} - \frac{2P}{l} & -\frac{7G}{2l^2} + \frac{P}{l} \\ -\frac{7G}{2l^2} + \frac{P}{l} & \frac{13G}{4l^2} - \frac{3P}{2l} \end{bmatrix} = \underbrace{\frac{G}{l^2} \begin{bmatrix} 5 & -\frac{7}{2} \\ -\frac{7}{2} & \frac{13}{4} \end{bmatrix}}_{[K_m]} + \underbrace{\frac{P}{l} \begin{bmatrix} -2 & 1 \\ 1 & -\frac{3}{2} \end{bmatrix}}_{[K_g]}.$$

⁷It is not possible to compute dD_1 and dD_2 simultaneously because the two equations of the system defined by (263) become linearly dependent for $P = P_{cr}$. This means that it is not possible to find the amplitude of the deformation, which reflects the fact that equilibrium is neutral in the critical phase.

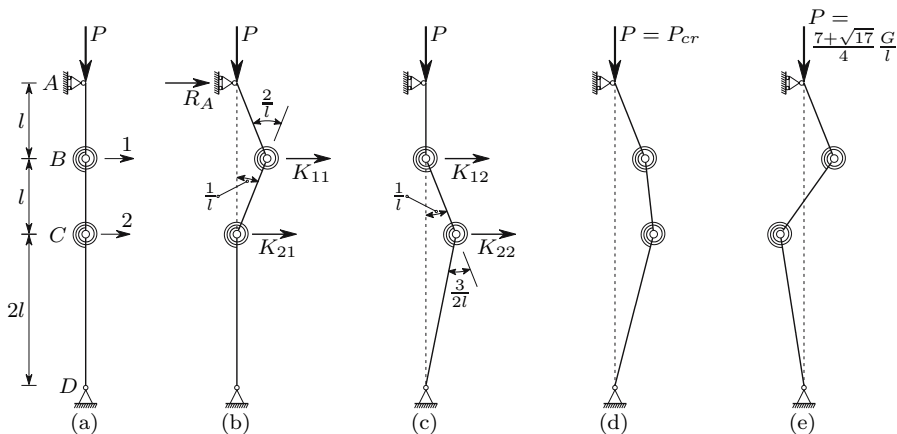


Fig. 173. Example of stability analysis in a column with bending stiffness

$[K_m]$ and $[K_g]$ represent the material and geometrical components of the stiffness matrix. The condition of a vanishing determinant yields the two values of P , for which equilibrium between the internal forces and P exists in a slightly deformed configuration

$$\begin{vmatrix} \frac{5G}{l^2} - \frac{2P}{l} & -\frac{7G}{2l^2} + \frac{P}{l} \\ -\frac{7G}{2l^2} + \frac{P}{l} & \frac{13G}{4l^2} - \frac{3P}{2l} \end{vmatrix} = 0 \Rightarrow P = \frac{7 - \sqrt{17} G}{4} \frac{G}{l} \quad \vee \quad P = \frac{7 + \sqrt{17} G}{4} \frac{G}{l} .$$

The critical load is thus $P_{cr} = \frac{7 - \sqrt{17} G}{4} \frac{G}{l}$. The equilibrium configurations which correspond to these two roots may be found in the same way as in the first example, yielding the vectors

$$P = P_{cr} = \frac{7 - \sqrt{17} G}{4} \frac{G}{l} \Rightarrow \begin{cases} dD_1 = 1 \\ dD_2 = 1.281 \end{cases}$$

and

$$P = \frac{7 + \sqrt{17} G}{4} \frac{G}{l} \Rightarrow \begin{cases} dD_1 = 1 \\ dD_2 = -0.781 \end{cases} .$$

The configurations corresponding to these two displacement-vectors are represented in Figs. 173-d and 173-e. Thus, when buckling occurs, the column deforms with the shape given in Fig. 173-d.

In structures with a high degree of kinematic indeterminacy the critical load and the buckling shapes are not computed in the same way as in the two simple examples analysed. Generally, a factor λ is required, by which the applied load must be multiplied in order to find the critical load. It may be shown that, if the material has linear elastic behaviour, if the displacements are small enough to be considered as infinitesimal, and if the displacement of a point of the structure may be expressed as a linear function of the displacements of the nodal points, as happens in the two simple examples above and

also in the most used finite-element discretizations, *the material stiffness is constant and the geometrical stiffness is proportional to the applied loads*. Under these conditions, the problem may be formulated as shown below ($\{dD\}$ is the vector containing the n kinematic unknowns and $\{0\}$ is a vector with n zeros)

$$\begin{aligned} [K] \{dD\} = \{0\} &\Rightarrow ([K_m] + \lambda [K_g]) \{dD\} = \{0\} \\ &\Rightarrow [K_m] \{dD\} = -\lambda [K_g] \{dD\} . \end{aligned} \quad (267)$$

The last equality in (267) may be reduced to the form of the algebraic *generalized symmetric eigenvalue problem*

$$[A] \{z\} = \lambda' [B] \{z\} , \quad (268)$$

where the matrices $[A]$ and $[B]$ are symmetrical and $[B]$ is positive definite. The matrices $[K_m]$ and $[K_g]$ are symmetrical. Furthermore, $[K_m]$ is positive definite. Thus, rearranging the last of 267, we may put it in the form corresponding to the generalized eigenvalue problem (268), that is

$$\begin{cases} [A] = [K_g] \\ [B] = [K_m] \\ \{z\} = \{dD\} \\ \lambda' = -\frac{1}{\lambda} \end{cases} \Rightarrow \begin{cases} [K_g] \{dD\} = -\frac{1}{\lambda} [K_m] \{dD\} \\ \Leftrightarrow [A] \{z\} = \lambda' [B] \{z\} . \end{cases}$$

The eigenvectors represent the buckling modes. The resolution of the two simple problems (Figs. 172 and 173) with this method is left as an exercise for the reader.

XI.6.c Framed Structures Under Bending

When the stability of a framed structure is guaranteed by the bending stiffness of its members, the computation of the critical load requires the stiffness of the bars to be expressed as functions of the corresponding axial forces. In this Sub-section we develop expressions to compute the stiffness matrix of a bar with four and three degrees of freedom, disregarding axial deformations (see Footnote 77), and assuming that the rotations are small (see the last part of Subsect. IX.1.b for an analysis of the error introduced by this assumption). The last part includes examples of both the determination of critical loads and of the approximate computation of displacements in framed structures, taking the interaction between internal forces and deformations into consideration.

XI.6.c.i Stiffness Matrix of a Compressed Bar

The stiffness matrix of a bar with the four degrees of freedom represented in Fig. 174-a may be found by integration of the differential equation which

defines the relations between forces applied in the coordinates and the bending moments, when the bending deformation is taken into account. To this end, let us consider the column represented in Fig. 174-b, under the action of the compressive axial force N , the transversal load V and the moment M . The differential equation of this problem may be established considering the curvature corresponding to the bending moment in the cross-section defined by coordinate z (Fig. 174-b).

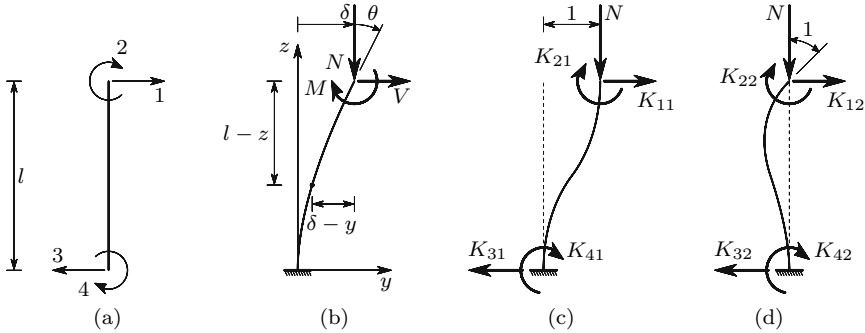


Fig. 174. Determination of the stiffness matrix of a compressed bar

Denoting by Δ the displacement of the upper cross-section (Fig. 174-b), we get

$$\frac{1}{\rho} = \frac{d^2y}{dz^2} = \frac{1}{EI} \overbrace{[M + N(\delta - y) + V(l - z)]}^{\text{bending moment}} \tag{269}$$

$$\Rightarrow \frac{d^2y}{dz^2} + \frac{N}{EI}y = \frac{1}{EI} [M + N\Delta + V(l - z)] .$$

We may easily verify that this equation admits the particular integral

$$y = \frac{M}{N} + \frac{V}{N} (l - z) + \delta .$$

Thus its general solution is

$$y = C_1 \cos(kz) + C_2 \sin(kz) + \frac{M}{N} + \frac{V}{N} (l - z) + \delta \quad \text{with} \quad k^2 = \frac{N}{EI} .$$

Derivating this expression with respect to z , we get the equation of the rotations

$$\frac{dy}{dz} = -kC_1 \sin(kz) + kC_2 \cos(kz) - \frac{V}{N} .$$

The support conditions in the built-in end allow the determination of the integration constants. Thus, we have

$$z = 0 \Rightarrow \begin{cases} y = 0 \Rightarrow C_1 = -\frac{M}{N} - \frac{Vl}{N} - \delta \\ \frac{dy}{dz} = 0 \Rightarrow kC_2 - \frac{V}{N} = 0 \Rightarrow C_2 = \frac{V}{kN} . \end{cases}$$

Substituting these values in the previous expressions, we get

$$\begin{aligned} y &= \frac{V}{kN} \sin(kz) - \left(\delta + \frac{M + Vl}{N} \right) \cos(kz) + \frac{M}{N} + \frac{V}{N} (l - z) + \delta \\ \frac{dy}{dz} &= \frac{V}{N} \cos(kz) + \left(\delta + \frac{M + Vl}{N} \right) k \sin(kz) - \frac{V}{N} . \end{aligned} \quad (270)$$

The displacement Δ and the rotation θ of the upper end of the column may be related to the applied forces, yielding

$$z = l \Rightarrow \begin{cases} y = \delta \Rightarrow \frac{V}{kN} \sin(kl) - \left(\delta + \frac{M + Vl}{N} \right) \cos(kl) + \frac{M}{N} + \delta = \delta \\ \frac{dy}{dz} = \theta \Rightarrow \frac{V}{N} \cos(kl) + \left(\delta + \frac{M + Vl}{N} \right) k \sin(kl) - \frac{V}{N} = \theta . \end{cases}$$

Rearranging this system of equations, the following form may be given to it

$$\begin{cases} \frac{k \sin(kl)}{N} M + \frac{kl \sin(kl) + \cos(kl) - 1}{N} V = \theta - \delta k \sin(kl) \\ \frac{1 - \cos(kl)}{N \cos(kl)} M + \frac{\tan(kl) - kl}{kN} V = \delta . \end{cases}$$

By solving this system of equations, we get the force V and the moment M required to introduce the displacement δ and the rotation θ in the upper cross-section, for a given value of the axial force N . This solution takes the form

$$M = \frac{c_1 b_2 - b_1 c_2}{a_1 b_2 - a_2 b_1} \quad V = \frac{a_1 c_2 - c_1 a_2}{a_1 b_2 - a_2 b_1} \quad (271)$$

with

$$\begin{aligned} a_1 &= \frac{k \sin(kl)}{N} & b_1 &= \frac{kl \sin(kl) + \cos(kl) - 1}{N} & c_1 &= \theta - \delta k \sin(kl) \\ a_2 &= \frac{1 - \cos(kl)}{N \cos(kl)} & b_2 &= \frac{\tan(kl) - kl}{kN} & c_2 &= \delta . \end{aligned}$$

From these expressions we get, after some manipulation,

$$\begin{aligned}
 a_1 b_2 - a_2 b_1 &= \frac{2 [1 - \cos(kl)] - kl \sin(kl)}{N^2 \cos(kl)} \\
 c_1 b_2 - b_1 c_2 &= \frac{\theta [\tan(kl) - kl] + \Delta [k - k \cos(kl) - k \sin(kl) \tan(kl)]}{kN} \quad (272) \\
 a_1 c_2 - c_1 a_2 &= \frac{\theta [\cos(kl) - 1] + \Delta k \sin(kl)}{N \cos(kl)} .
 \end{aligned}$$

The same line of reasoning as used in the first example in Subject. XI.6.b (264), leads to the conclusion that the elements K_{11} and K_{21} of the stiffness matrix are the transversal force V and the moment M required to induce the deformation represented in Fig. 174-c, i.e., $\delta = 1$ and $\theta = 0$. Substituting these values in (272) and the result of this substitution in (271), we get

$$\begin{aligned}
 V = K_{11} &= \frac{N}{2 - 2 \cos(kl) - kl \sin(kl)} k \sin(kl) \\
 M = K_{21} &= \frac{N}{2 - 2 \cos(kl) - kl \sin(kl)} [\cos(kl) - 1] .
 \end{aligned}$$

Elements K_{31} and K_{41} may then be found by means of equilibrium considerations, yielding

$$K_{31} = K_{11} \quad \text{and} \quad K_{41} = -K_{11}l - K_{21} - N = K_{21} .$$

The last equality is obtained by a moment equation with respect to the built-in end. The antisymmetry of the deformation also leads directly to this equality.

The elements K_{12} and K_{22} are the transversal force V and the moment M needed to induce the deformation represented in Fig. 174-d, i.e., $\delta = 0$ and $\theta = 1$. The same procedure as above leads to

$$\begin{aligned}
 V = K_{12} &= \frac{N}{2 - 2 \cos(kl) - kl \sin(kl)} [\cos(kl) - 1] = K_{21} \\
 M = K_{22} &= \frac{N}{2 - 2 \cos(kl) - kl \sin(kl)} \frac{\sin(kl) - kl \cos(kl)}{k} .
 \end{aligned}$$

Elements K_{32} and K_{42} also obtained by means of equilibrium considerations, which yield

$$K_{32} = K_{12} \quad \text{and} \quad K_{42} = -K_{22} - K_{12}l = \frac{N}{2 - 2 \cos(kl) - kl \sin(kl)} \frac{kl - \sin(kl)}{k} .$$

The two remaining columns of the stiffness matrix could be obtained by considering unit displacements in coordinates 3 and 4. It is, however, obvious that the results would be the same as those obtained by interchanging the roles of

indices 1 and 2 with indices 3 and 4, respectively. Thus, the complete stiffness matrix takes the form

$$[K] = \frac{N}{2 - 2 \cos(kl) - kl \sin(kl)} \times \begin{bmatrix} k \sin(kl) & \cos(kl) - 1 & k \sin(kl) & \cos(kl) - 1 \\ \cos(kl) - 1 & \frac{\sin(kl) - kl \cos(kl)}{k} & \cos(kl) - 1 & \frac{kl - \sin(kl)}{k} \\ k \sin(kl) & \cos(kl) - 1 & k \sin(kl) & \cos(kl) - 1 \\ \cos(kl) - 1 & \frac{kl - \sin(kl)}{k} & \cos(kl) - 1 & \frac{\sin(kl) - kl \cos(kl)}{k} \end{bmatrix}. \quad (273)$$

Sometimes it is also useful to know the stiffness matrix of a compressed bar with the three coordinates represented in Fig. 175-a.

The corresponding stiffness coefficients may easily be obtained by solving the problems represented in Figs. 175-b and 175-c. Since these problems do not have any additional difficulty compared with those in Fig. 174, their detailed analysis is left as an exercise to the reader. The resulting stiffness matrix takes the form

$$\frac{N}{\sin(kl) - kl \cos(kl)} \begin{bmatrix} k \cos(kl) & -\sin(kl) & k \cos(kl) \\ -\sin(kl) & l \sin(kl) & -\sin(kl) \\ k \cos(kl) & -\sin(kl) & k \cos(kl) \end{bmatrix}. \quad (274)$$

All examples of determination of the critical load presented in Sect. XI.3, and also examples XI.11, XI.12 and XI.13, may easily be confirmed by analysing particular elements of the two stiffness matrices above (273) and (274).

Thus, the critical load of a pin-ended bar (Euler's problem) is attained when coefficient K_{22} of the matrix in (274) vanishes, that is, when the bar ceases to have sufficient stiffness to resist the rotation of the upper cross-section. The smallest non-zero value of kl for which this coefficient vanishes is π , which coincides with Euler's solution.

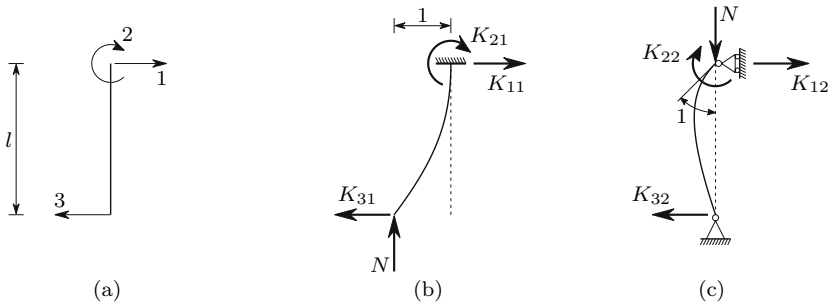


Fig. 175. Determination of the stiffness matrix of a bar with three coordinates

The critical load of the example presented in Fig. 166-a is attained when coefficient K_{33} of the matrix in (274) vanishes, which takes place for $\cos(kl) = 0$, i.e., when the condition $kl = (2n - 1) \frac{\pi}{2}$ is satisfied, which leads to the effective length $2l$.

The critical load of the example in Fig. 166-b corresponds to a vanishing value of coefficient K_{11} of (273), which takes place for $\sin(kl) = 0$.

In the example of Fig. 166-c the critical load is reached when the bar loses the stiffness needed to resist the transversal displacement of the mid-height cross-section. Considering the column to be divided in two bars with equal length $\frac{l}{2}$, the horizontal stiffness of the column in the connection point between the two bars is given by twice the coefficient K_{11} of (273), with the length of the bar reduced to $\frac{l}{2}$. Thus, buckling takes place when $\sin(k\frac{l}{2}) = 0$, that is, when $k\frac{l}{2} = \pi$.

The critical load of the column depicted in Fig. 166-d is attained when the coefficient K_{22} in (273) vanishes, which happens for $\sin(kl) = kl \cos(kl)$. This is exactly the expression used in Subsect. XI.3.c to find the effective length of this column.

In example XI.11 the rotational stiffness of cross-section B has two components, one corresponding to the deformation of column segment BC and other corresponding to the rotation of the rigid segment AB . The first component is given by coefficient K_{22} of the matrix in (274). The second takes the value $-Pl'$, since, for a unit rotation θ , this is the moment needed in cross-section B , to balance the moment caused by the load P . Thus, the total rotational stiffness of cross-section B vanishes when the following condition is satisfied

$$K = \frac{Pl \sin(kl)}{\sin(kl) - kl \cos(kl)} - Pl' = 0 \Rightarrow l' \cos(kl) + \frac{l - l'}{kl} \sin(kl) = 0 ,$$

which coincides with the expression obtained in example XI.11.

Also in example XI.12, the horizontal stiffness of the column in point B has two components, one corresponds to the deformation of segment BC and the other is the force needed to balance the horizontal component of the pinned bar AB , when point B suffers a unit displacement. The first component coincides with coefficient K_{33} of the matrix in (274). The second component takes the value $-\frac{P}{l'}$. Buckling occurs when the total stiffness vanishes, that is, when the following condition is satisfied

$$K = \frac{Pk \cos(kl)}{\sin(kl) - kl \cos(kl)} - \frac{P}{l'} = 0 \Rightarrow \left(1 + \frac{l'}{l}\right) kl = \tan(kl) .$$

Finally, in example XI.13 the rotational stiffness of cross-section B has the components which correspond to the deformation of segments AB and BC . These components are given by coefficient K_{22} of the matrix in (274), with the lengths l and l' , respectively. The critical load may thus be obtained by solving the equation

$$K = \frac{Pl \sin(kl)}{\sin(kl) - kl \cos(kl)} + \frac{Pl' \sin(kl')}{\sin(kl') - kl' \cos(kl')} = 0 .$$

This expression defines the problem completely, as opposed to the equation obtained in example XI.13. In fact, if we have $l = l'$, we can see immediately that $\sin(kl) = 0 \Rightarrow kl = n\pi$ is a solution of the equation. The expression found in XI.13 may be obtained from this one by dividing both terms (numerator and denominator) of the fraction representing the first component by $\sin(kl)$ and both terms of the second component by $\sin(kl')$. When we have $l = l'$, this operation eliminates the roots of the equation that are defined by $kl = n\pi$.

XI.6.c.ii Stiffness Matrix of a Tensioned Bar

The stiffness of a tensioned bar with the degrees of freedom represented in Fig. 174-a may be obtained in the same way as in the case of the compressed bar. The differential equation defining the relations between the forces applied in the coordinates and the bending moments, when a tensile force is considered, takes a similar form to (269), but with a reversed sign in the elements containing N (Fig. 174-b with N pointing upwards)

$$\begin{aligned} \frac{1}{\rho} &= \frac{d^2y}{dz^2} = \frac{1}{EI} [M - N(\delta - y) + V(l - z)] \\ \Rightarrow \frac{d^2y}{dz^2} - \frac{N}{EI}y &= \frac{1}{EI} [M - N\delta + V(l - z)]. \end{aligned}$$

This equation admits the particular integral

$$y = \delta - \frac{M}{N} - \frac{V}{N}(l - z),$$

Since in this case the homogeneous equation does not have imaginary roots, its general solution takes the form

$$y = C_1 e^{kz} + C_2 e^{-kz} + \delta - \frac{M}{N} - \frac{V}{N}(l - z) \quad \text{with} \quad k^2 = \frac{N}{EI}. \quad (275)$$

In the same way as in the case of axial compression, the integration constants may be eliminated by means of the support conditions in the built-in end (Fig. 174-b). In this case we have

$$z = 0 \Rightarrow \begin{cases} y = 0 \Rightarrow C_1 + C_2 + \delta - \frac{M}{N} - \frac{Vl}{N} = 0 \\ \frac{dy}{dz} = 0 \Rightarrow kC_1 - kC_2 + \frac{V}{N} = 0. \end{cases}$$

Solving this system of equations, we get

$$C_1 = \frac{M}{2N} - \frac{V}{2kN} + \frac{Vl}{2N} - \frac{\delta}{2} \quad \text{and} \quad C_2 = \frac{M}{2N} + \frac{V}{2kN} + \frac{Vl}{2N} - \frac{\delta}{2}.$$

Substituting these expressions in the general solution (275) and using the definitions of hyperbolic sine and cosine ($\sinh x = \frac{e^x - e^{-x}}{2}$, $\cosh x = \frac{e^x + e^{-x}}{2}$), we may give (275) the following form

$$y = \left(\frac{M + Vl}{N} - \delta \right) \cosh(kz) - \frac{V}{kN} \sinh(kz) + \delta - \frac{M}{N} - \frac{V}{N} (l - z) .$$

Derivating with respect to z , we get

$$\frac{dy}{dz} = \left(\frac{M + Vl}{N} - \delta \right) k \sinh(kz) - \frac{V}{N} \cosh(kz) + \frac{V}{N} .$$

These two expressions are very similar to those obtained in the compressive case (270), showing, in addition to the substitution of sine by hyperbolic sine and of cosine by hyperbolic cosine, only sign differences in some elements. The treatment of these expressions until the stiffness coefficients are obtained is the same as in the case of axial compression, so it is not repeated here. The resulting stiffness matrix takes the form

$$[K] = \frac{N}{2 - 2 \cosh(kl) + kl \sinh(kl)} \times \begin{bmatrix} k \sinh(kl) & 1 - \cosh(kl) & k \sinh(kl) & 1 - \cosh(kl) \\ 1 - \cosh(kl) & \frac{kl \cosh(kl) - \sinh(kl)}{k} & 1 - \cosh(kl) & \frac{\sinh(kl) - kl}{k} \\ k \sinh(kl) & 1 - \cosh(kl) & k \sinh(kl) & 1 - \cosh(kl) \\ 1 - \cosh(kl) & \frac{\sinh(kl) - kl}{k} & 1 - \cosh(kl) & \frac{kl \cosh(kl) - \sinh(kl)}{k} \end{bmatrix} . \tag{276}$$

In the case of the coordinates defined in Fig. 175-a the stiffness matrix for a tensile axial force takes the form

$$[K] = \frac{N}{kl \cosh(kl) - \sinh(kl)} \begin{bmatrix} k \cosh(kl) & -\sinh(kl) & k \cosh(kl) \\ -\sinh(kl) & l \sinh(kl) & -\sinh(kl) \\ k \cosh(kl) & -\sinh(kl) & k \cosh(kl) \end{bmatrix} . \tag{277}$$

XI.6.c.iii Linearization of the Stiffness Coefficients

The stiffness matrices defined by (273), (274), (276) and (277) include the influences of the bending stiffness (by means of the term EI contained in k) and of the axial force. However, the stiffness coefficients are not used in this form, as a rule, since the fact that it is not possible to decompose these matrices in a component which is independent of the axial force (the material stiffness), and in a component which is independent of the elasticity modulus of the material the bar is made of (the geometrical stiffness), prevents the use

of the algorithm based on the reduction of the problem to eigenvalue form (267).⁸

This problem may be circumvented by linearizing the stiffness coefficients. This may be achieved by computing the value of these coefficients and their derivatives with respect to the axial force, for a vanishing axial force. These operations are rather lengthy, since the elements of the stiffness matrices and their derivatives become indeterminate for $k = 0$. However, by using a computational program for symbolic manipulation, this virtually ceases to be a problem. Performing these operations in the expressions relating to compression (273) and (274) and tension (276) and (277), we conclude that the functions expressing the stiffness coefficients and their derivatives are continuous in the point defined by a vanishing axial force. For example, in the case of coefficient K_{11} in (273) and (276) we get

$$\begin{aligned} \lim_{N \rightarrow 0} \left[\frac{N}{2 - 2 \cos(kl) - kl \sin(kl)} k \sin(kl) \right] &= \frac{12EI}{l^3} \\ \lim_{N \rightarrow 0} \left[\frac{N}{2 - 2 \cosh(kl) + kl \sinh(kl)} k \sinh(kl) \right] &= \frac{12EI}{l^3} \\ \lim_{N \rightarrow 0} \left\{ \frac{d}{dN} \left[\frac{N}{2 - 2 \cos(kl) - kl \sin(kl)} k \sin(kl) \right] \right\} &= -\frac{6}{5l} \\ \lim_{N \rightarrow 0} \left\{ \frac{d}{dN} \left[\frac{N}{2 - 2 \cosh(kl) + kl \sinh(kl)} k \sinh(kl) \right] \right\} &= \frac{6}{5l}. \end{aligned}$$

The difference in the sign between the two last expressions is a consequence of the fact that in the first one a compressive axial force is considered to be positive, while in the second one the tensile force is positive. The linearized form of this coefficient is then (a tensile axial force is considered as positive)

$$K_{11} = \frac{12EI}{l^3} + N \frac{6}{5l}.$$

Carrying out the same operations for all the stiffness coefficients, the following matrices are obtained

$$[K] = EI \begin{bmatrix} \frac{12}{l^3} & -\frac{6}{l^2} & \frac{12}{l^3} & -\frac{6}{l^2} \\ -\frac{6}{l^2} & \frac{4}{l} & -\frac{6}{l^2} & \frac{2}{l} \\ \frac{12}{l^3} & -\frac{6}{l^2} & \frac{12}{l^3} & -\frac{6}{l^2} \\ -\frac{6}{l^2} & \frac{2}{l} & -\frac{6}{l^2} & \frac{4}{l} \end{bmatrix} + N \begin{bmatrix} \frac{6}{5l} & -\frac{1}{10} & \frac{6}{5l} & -\frac{1}{10} \\ -\frac{1}{10} & \frac{2l}{15} & -\frac{1}{10} & -\frac{l}{30} \\ \frac{6}{5l} & -\frac{1}{10} & \frac{6}{5l} & -\frac{1}{10} \\ -\frac{1}{10} & -\frac{l}{30} & -\frac{1}{10} & \frac{2l}{15} \end{bmatrix} \quad (278)$$

and

$$[K] = EI \begin{bmatrix} \frac{3}{l^3} & -\frac{3}{l^2} & \frac{3}{l^3} \\ -\frac{3}{l^2} & \frac{3}{l} & -\frac{3}{l^2} \\ \frac{3}{l^3} & -\frac{3}{l^2} & \frac{3}{l^3} \end{bmatrix} + N \begin{bmatrix} \frac{6}{5l} & -\frac{1}{5} & \frac{6}{5l} \\ -\frac{1}{5} & \frac{l}{5} & -\frac{1}{5} \\ \frac{6}{5l} & -\frac{1}{5} & \frac{6}{5l} \end{bmatrix}, \quad (279)$$

⁸In this problem the displacement of a point of the bar is not a linear function of the displacements of the coordinates, as required for (267) to be valid.

respectively for the coordinates indicated in Figs. 174-a and 175-a. The first elements in each equation represent the material stiffness (proportional to the elasticity modulus E) and the second ones are the geometrical stiffness (proportional to the axial force N).

In Fig. 176 the exact and linearized forms of coefficient K_{11} of the first matrix, as functions of N , are represented. The infinite peaks appearing in the compressive part of the first diagram correspond to the values of kl for which the denominator $2 - 2 \cos(kl) - kl \sin(kl)$ (273) vanishes. However, the very high values of the stiffness coefficients do not have a physical correspondence. In fact, the above theory is only valid for small rotations, since only under these conditions may we accept that $\frac{1}{\rho} = \frac{d^2y}{dz^2}$ (see the last part of Subject. IX.1.b). When the quantity $2 - 2 \cos(kl) - kl \sin(kl)$ gets close to zero, the stiffness coefficients take high values, which leads to high rotation values, as may be concluded from the second of (270) (M and V take the values of the stiffness coefficients).

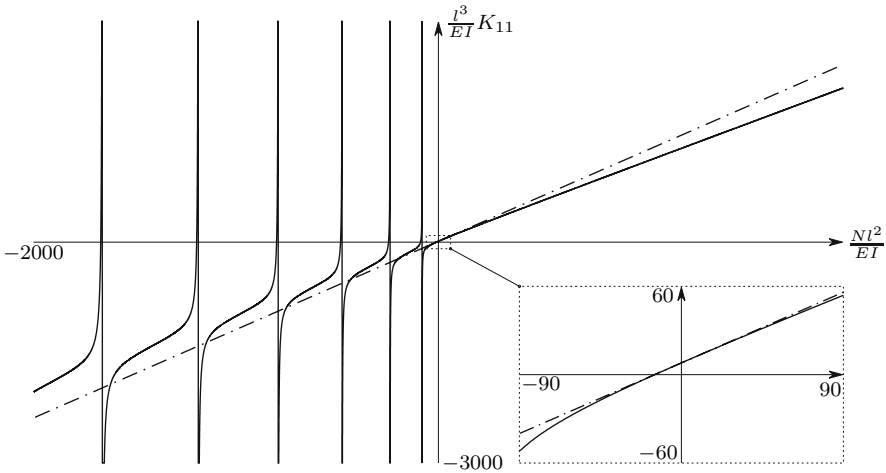


Fig. 176. “Exact” (solid lines) and linearized (dashed-dotted line) forms of stiffness coefficient K_{11} (Fig. 174-a)

Obviously, the linearization of the stiffness coefficient introduces errors into the computation of buckling forces and shapes. However, these errors are not large if only the critical load and the first buckling mode are required, and if the kinematic coordinates are well-chosen. In the case of higher modes, considerable errors may be introduced.

When the stiffness coefficients are used in their exact form (273), (274), (276) and (277), we get an infinite number of buckling modes. As a consequence of the linearization, the number of buckling modes obtained becomes

equal to the degree of kinematic indeterminacy, as may be concluded from the algebraic form of the problem (267).

When the linearized form of the stiffness coefficients is used, the correct choice of the kinematic coordinates is very important, since local buckling modes may only be captured with sufficient accuracy if the chosen coordinates allow it. For this reason, in a systematic computational analysis it is advisable to consider additional nodes in the middle or even in each third of the bars, although these nodes are not needed to compute the internal forces.

In Subsect. XI.6.c.iv examples are presented to illustrate these considerations.

XI.6.c.iv Examples of Application

As a first example of stability analysis of a framed structure using the displacement method, let us consider the plane frame represented in Fig. 177-a.

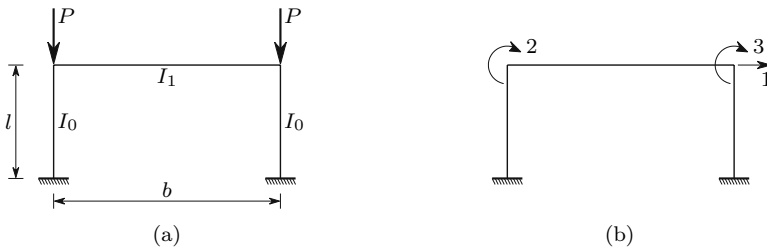


Fig. 177. Stability analysis of a plane frame

This problem has an analytical solution which may be compared with the solution yielded by the displacement method, both in the exact and in the linearized formulation. This solution is defined by the expression (see, e.g., [11], Sect. 2.4)

$$\frac{kl}{\tan(kl)} = -\frac{6lI_1}{bI_0} \quad \text{with} \quad k = \sqrt{\frac{P}{EI_0}} .$$

Giving numerical values to the geometrical parameters, we get the critical load ($E = 206 \text{ GPa}$)

$$\begin{aligned} l &= 5m \\ b &= 10m \\ I_0 &= 20 \times 10^{-6} m^4 \\ I_1 &= 50 \times 10^{-6} m^4 \end{aligned} \Rightarrow \left\{ \begin{aligned} \frac{kl}{\tan(kl)} &= -7.5 \Rightarrow kl = 2.785931 \\ \Rightarrow P_{cr} &= (kl)^2 \frac{EI_0}{l^2} = 1279081N = 1279.081kN . \end{aligned} \right.$$

To resolve this problem by means of the displacement method, the coordinates represented in Fig. 177-b may be used. Denoting by K^0 and K^1 the stiffness coefficients of the vertical and horizontal bars, respectively (Fig. 174-a),

we conclude immediately that the forces required to introduce the deformation depicted in Fig. 178-a ($D_1 = 1, D_2 = D_3 = 0$) take the values

$$K_{11} = 2K_{11}^0 \quad K_{21} = K_{12}^0 \quad K_{31} = K_{12}^0 .$$

Proceeding in the same way in the configurations represented in Figs. 178-b ($D_2 = 1, D_1 = D_3 = 0$) and 178-c ($D_1 = D_2 = 0, D_3 = 1$), we get the other elements of the stiffness matrix of this structure, which takes the form

$$[K] = \begin{bmatrix} K_{11} & K_{12} & K_{13} \\ K_{21} & K_{22} & K_{23} \\ K_{31} & K_{32} & K_{33} \end{bmatrix} = \begin{bmatrix} 2K_{11}^0 & K_{12}^0 & K_{12}^0 \\ K_{12}^0 & K_{22}^0 + K_{22}^1 & K_{24}^1 \\ K_{12}^0 & K_{24}^1 & K_{22}^0 + K_{22}^1 \end{bmatrix} .$$

The critical load is the smallest value of P which makes this matrix singular ($|K| = 0$).

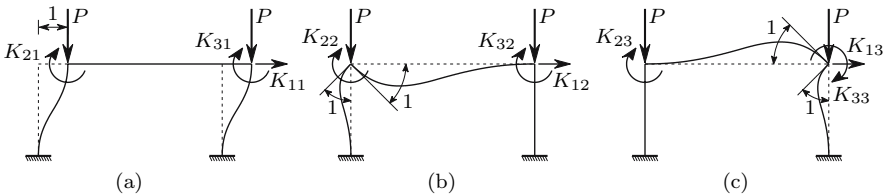


Fig. 178. Elements of the stiffness matrix

Writing a small computer program with the expression of the determinant of matrix $[K]$, taking the stiffness coefficients K^0 from (273) and the coefficients K^1 from the first matrix of (278) (the elements of (273) become indeterminate for $N = 0$), we conclude that the smallest value of P that leads to a vanishing determinant coincides with the above solution. When the linearized form of the stiffness coefficients is used (278), we get the slightly higher value P_{cr}^l

$$P_{cr}^l = 1290528N = 1290.528kN \Rightarrow \frac{P_{cr}^l}{P_{cr}} = \frac{1290.528}{1279.081} = 1.0089 .$$

The first buckling mode is defined by the displacement vector that satisfies the condition

$$[K] \{D\} = \{0\} \quad \text{with} \quad P = P_{cr} \Rightarrow |K| = 0 .$$

Since we have only three coordinates, the components of vector $\{D\}$ may be computed by means of the same algorithm that has been used in the resolution of exercise II.1. Thus, using the same line of reasoning as described there, we easily conclude that a vector with the components

$$D_1 = \begin{vmatrix} K_{12} & K_{13} \\ K_{22} & K_{23} \end{vmatrix} \quad D_2 = - \begin{vmatrix} K_{11} & K_{13} \\ K_{21} & K_{23} \end{vmatrix} \quad D_3 = \begin{vmatrix} K_{11} & K_{12} \\ K_{21} & K_{22} \end{vmatrix}$$

satisfies the equation above. The results obtained with these expressions are practically the same, either taking the exact stiffness coefficients ((273), or the linearized form (278). Multiplying the elements of this vector by a constant, so that the displacement D_1 takes the value of 10 cm, we get for the rotations $D_2 = D_3 = 0.010$ radians. This buckling mode corresponds to the deformed configuration represented in Fig. 179-a.

When the load corresponding to the second buckling mode is computed, very different values are obtained from the exact and linearized forms of the stiffness coefficients. Thus, using (273) we get $P = 4304kN$, while (278) gives $P = 8034kN$. However, the corresponding buckling modes are similar, defining the configuration represented in Fig. 179-b.

To illustrate the correct choice of the kinematic coordinates, when the linearized form of the stiffness coefficients is used, let us consider the plane structure represented in Fig. 180-a, where the horizontal and vertical bars have cross-sections with moments of inertia $5I$ and I , respectively.

Since, when buckling occurs, a rotation of node B takes place, the corresponding stiffness may be used to compute the critical value of load P . The rotational stiffness of node B is the moment K which is needed to cause a unit rotation of the ends of the bars converging in node B , that is, it is the sum of

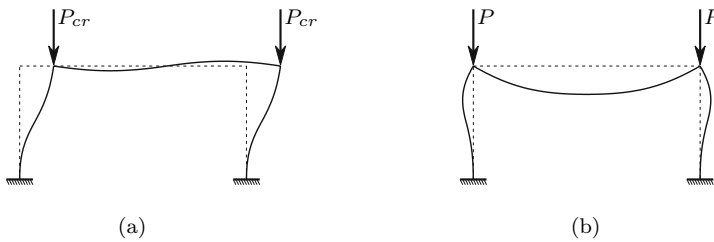


Fig. 179. First and second buckling modes of the frame represented in Fig. 177-a

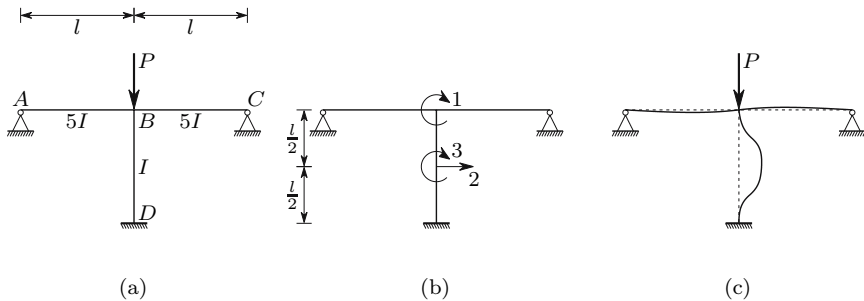


Fig. 180. Example illustrating the importance of the correct choice of the kinematic coordinates, when the linearized form of the stiffness coefficients is used

the stiffness coefficients K_{22} both in the case represented in Fig. 174-a for the vertical bar, and in the case represented in Fig. 175-a for the horizontal bars. Thus, we get from the first matrix in (279) (horizontal bars, $N = 0$) and from (273) (vertical bar)

$$K = 2 \times \frac{3E5I}{l} + \frac{P}{k} \frac{\sin(kl) - kl \cos(kl)}{2 - 2 \cos(kl) - kl \sin(kl)}.$$

Since we have $P = k^2 EI$, we may give this expression the following form

$$K = \frac{EI}{l} \left[30 + kl \frac{\sin(kl) - kl \cos(kl)}{2 - 2 \cos(kl) - kl \sin(kl)} \right].$$

A simple numerical investigation shows that the smallest value of load P that leads to a vanishing value of this stiffness is

$$K = 0 \Rightarrow kl = 6.083065 \Rightarrow P = P_{cr} = 37.00368 \frac{EI}{l^2}. \quad (280)$$

Repeating this analysis with the linearized form of the stiffness coefficients of the bars, we get from (278) and (279)

$$K = 2 \times \frac{3E5I}{l} + \frac{4EI}{l} - P \frac{2l}{15} = 0 \Rightarrow P = 255 \frac{EI}{l^2}.$$

We find that the solution yielded by the linearized form of the stiffness coefficients leads to an enormous error.

However, if instead of considering only the rotation coordinate in node B , we consider the stiffness matrix corresponding to the three coordinates represented in Fig. 180-b, the results obtained using the linearized forms of the stiffness coefficients come much closer to the exact solution. The procedure leading to the computation of the critical load and the first buckling mode is the same as in the case of the frame represented in Fig. 177, so it is not described here. The critical load computed using the exact form of the stiffness coefficients confirms the value given in (280). The linearized stiffness yields the value $P_{cr} = 37.453265 \frac{EI}{l^2}$. The error of this solution is approximately 1%. The displacement vector corresponding to this load shows that instability is caused almost exclusively by the buckling of the vertical bar: If we multiply the displacement vector corresponding to the first buckling mode by a constant factor, so that we get $D_2 = \frac{l}{10}$, we get for the rotations D_1 and D_3 the values -0.06035 radians (-3.4578°) and 0.025357 radians (1.4528°), respectively. Figure 180-c shows the deformed configuration represented by this displacement vector.

The fact that the rotation of node B plays a small role in the buckling of the structure is confirmed by an approximate computation of the critical load in which a vanishing rotation of node B is assumed. Under this condition, the buckling load of the vertical bar may be computed with Euler's formula, considering an effective length $l_e = \frac{l}{2}$, which yields the value

$$P_{cr} = \frac{\pi^2 EI}{\left(\frac{l}{2}\right)^2} = 39.47842 \frac{EI}{l^2} .$$

It is the fact that this buckling mode, which has a very local character, cannot be accurately described by a rotation coordinate in node B that leads to the large error of the linearized solution. However, this fact does not affect the accuracy of the solution yielded by the exact form of the stiffness coefficients.

In the two examples above the geometrical component of the stiffness matrix has been used to compute the critical load. The next example illustrates the influence of the geometrical stiffness on the correct computation of the displacements of frames with heavily compressed members. An example of considerable practical interest is the computation of the displacements caused by horizontal forces in frames with large compressive axial forces in their vertical members. To this end let us consider the same frame that was considered in the first example (Fig. 177), now under the action of the forces represented in Fig. 181-a.

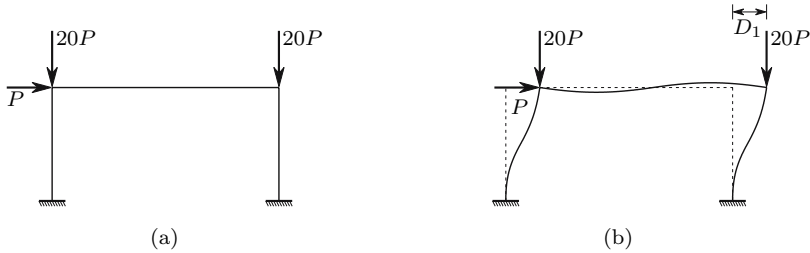


Fig. 181. Computation of the deformations caused by a horizontal load in a frame

As mentioned at the beginning of Subsect. XI.6.b, to introduce a deformation into a structure, which is represented by a given set of displacements in chosen kinematic coordinates, a set of forces must be applied at the same coordinate set. These forces are, therefore, functions of the given displacements. In the case of a system with three degrees of freedom, like the structure represented in Fig. 181, these functions may be expressed by

$$\begin{aligned} F_1 &= F_1 (D_1, D_2, D_3) \\ F_2 &= F_2 (D_1, D_2, D_3) \\ F_3 &= F_3 (D_1, D_2, D_3) . \end{aligned}$$

Conversely, a set of forces P_1, P_2, P_3 applied at the same coordinates introduces a set of displacements, D_1, D_2, D_3 , which must satisfy the conditions

$$\begin{aligned} F_1 (D_1, D_2, D_3) &= P_1 \\ F_2 (D_1, D_2, D_3) &= P_2 \\ F_3 (D_1, D_2, D_3) &= P_3 , \end{aligned}$$

which represent the equilibrium conditions between internal and external forces. In order to compute the values of D_1, D_2, D_3 it is therefore necessary to solve this system of equations, which is not linear, when the geometrical stiffness is considered. One of the most effective methods for solving non-linear systems of equations is the Newton-Raphson method. According to this method, given a set of estimated solutions, $\{D_1, D_2, D_3\}_i$, another set with improved approximation, $\{D_1, D_2, D_3\}_{i+1}$, may be computed by means of the algorithm

$$\underbrace{\begin{Bmatrix} D_1 \\ D_2 \\ D_3 \end{Bmatrix}}_{\{D\}_{i+1}} = \underbrace{\begin{Bmatrix} D_1 \\ D_2 \\ D_3 \end{Bmatrix}}_{\{D\}_i} + \underbrace{\begin{bmatrix} \frac{\partial F_1}{\partial D_1} & \frac{\partial F_1}{\partial D_2} & \frac{\partial F_1}{\partial D_3} \\ \frac{\partial F_2}{\partial D_1} & \frac{\partial F_2}{\partial D_2} & \frac{\partial F_2}{\partial D_3} \\ \frac{\partial F_3}{\partial D_1} & \frac{\partial F_3}{\partial D_2} & \frac{\partial F_3}{\partial D_3} \end{bmatrix}^{-1}}_{[K]_i^{-1}} \underbrace{\begin{Bmatrix} P_1 - F_{1i} \\ P_2 - F_{2i} \\ P_3 - F_{3i} \end{Bmatrix}}_{\{P-F\}_i},$$

where F_{1i}, F_{2i}, F_{3i} are the forces that must be applied at the coordinates in order to introduce the displacements $\{D_1, D_2, D_3\}_i$. Since, for small rotations and constant axial forces, the nodal forces are linear functions of the displacements, as shown by (271) and (272,) those forces may be computed by means of the matrix operation

$$\underbrace{\begin{Bmatrix} F_1 \\ F_2 \\ F_3 \end{Bmatrix}}_{\{F\}_i} = \underbrace{\begin{bmatrix} \frac{\partial F_1}{\partial D_1} = K_{11} & \frac{\partial F_1}{\partial D_2} = K_{12} & \frac{\partial F_1}{\partial D_3} = K_{13} \\ \frac{\partial F_2}{\partial D_1} = K_{21} & \frac{\partial F_2}{\partial D_2} = K_{22} & \frac{\partial F_2}{\partial D_3} = K_{23} \\ \frac{\partial F_3}{\partial D_1} = K_{31} & \frac{\partial F_3}{\partial D_2} = K_{32} & \frac{\partial F_3}{\partial D_3} = K_{33} \end{bmatrix}}_{[K]_i} \underbrace{\begin{Bmatrix} D_1 \\ D_2 \\ D_3 \end{Bmatrix}}_{\{D\}_i},$$

provided that the axial forces corresponding to the displacements $\{D\}_i$ are used to compute the derivatives. Matrix $[K]_i$ coincides with the definition of the stiffness matrix and depends on the axial forces installed in the bars. Vector $\{P\}$ has the components $P_1 = P$ and $P_2 = P_3 = 0$, since the vertical forces are directly balanced by the axial forces in the vertical bars, and so they do not need forces in the coordinates to be balanced.

The axial forces in the bars also depend on the displacements in the kinematic coordinates (Fig. 177-b). Thus, the axial force in the left vertical bar depends on the load $20P$ and on the shear force at the left end of the horizontal bar. This force depends on displacements D_2 and D_3 . Applying the same line of reasoning to the other two bars, and assuming that the displacements may be considered as infinitesimal, we conclude that the axial forces in the

P (N)	D_1 (cm) (exact stiffness)	D_1 (cm) (linearized stiffness)	D_1 (cm) (linear analysis)
1 000	0.17373	0.17373	0.17103
2 000	0.35303	0.35301	0.34207
5 000	0.92709	0.92705	0.85507
10 000	2.0247	2.0243	1.7103
20 000	4.9645	4.9588	3.4207
30 000	9.6289	9.5960	5.1310
40 000	18.182	18.024	6.8413
50 000	39.009	38.091	8.5517
55 000	66.855	63.925	9.4068
60 000	161.26	144.31	10.262
65 000	–	–	11.117

left (N_l), horizontal (N_h) and right (N_r) bars take the values given by the expressions

$$\begin{cases} N_l = -20P - K_{12}^1 D_2 - K_{14}^1 D_3 \\ N_h = -P + K_{11}^0 D_1 + K_{12}^0 D_2 \\ N_r = -20P + K_{32}^1 D_2 + K_{34}^1 D_3 , \end{cases}$$

where K^0 and K^1 represent the same quantities as in the first example (Figs. 177 and 178) and are obtained from the previous iteration ($i - 1$). Once the axial forces are defined, the new stiffness coefficients may be computed.

The iterative procedure may be summarized by the following scheme

$$\{D\}_i \rightarrow \begin{cases} N_l, N_h, N_r \rightarrow [K]_i \\ \{F\}_i \end{cases} \rightarrow \{D\}_{i+1} = \{D\}_i + [K]_i^{-1} \{P - F\}_i .$$

The process converges in a very small number of iterations, which depends on the importance of the geometrical stiffness. In the following Table the results obtained for the horizontal displacement D_1 (Fig. 181-b) are presented, considering several values of P and the following alternatives for the stiffness coefficients: exact form (2nd column), linearized form (3rd column) and constant values, i.e., no geometrical stiffness (4th column)

When the geometrical stiffness is considered it is not possible to find the displacement corresponding to the last value of P , since it is larger than the critical load of the structure yielded by the procedure presented here (see final comment). This load is slightly smaller than that computed in the example without the horizontal load, which is because this load introduces a compression in the horizontal bar and increases the axial force in the right vertical bar. The determinant of the stiffness matrix of this structure vanishes during the iterative process when the load exceeds the value

$$P_{cr} = 63132N \Rightarrow 20P_{cr} = 1262640N .$$

This value has been computed using the exact form of the stiffness coefficients. If the linearized form is used instead, the value $P_{cr} = 63804N$ is obtained.

In most framed structures the displacements are relatively small, so the influence of the deformation in the distribution of axial forces is also small. For this reason, an insignificant error is generally introduced if the iterative procedure described above is replaced by a direct computation, assuming that the axial forces remain constant and equal to the values yielded by a linear computation. This procedure reduces the non-linear problem to a sequence of two linear problems: the usual linear computation of the axial forces disregarding the effect of the geometrical stiffness, followed by another linear computation, in which the displacements are computed by means of a corrected stiffness matrix, where the influence of the axial forces (computed in the first step) in the stiffness is taken into consideration. An even simpler alternative is to take the axial forces obtained by locking the kinematic coordinates, when the bars are considered as axially non-deformable.

Applying the latter alternative to the present problem, we have $N_l = -20P$, $N_r = -20P$ and $N_h = -P$. Determining the stiffness matrix which corresponds to these axial forces, we get the following values of displacement D_1

P (N)	D_1 (cm) (exact stiffness)	D_1 (cm) (linearized stiffness)
1 000	0.17373	0.17373
2 000	0.35303	0.35303
5 000	0.92719	0.92714
10 000	2.0252	2.0247
20 000	4.9672	4.9614
30 000	9.6389	9.6058
40 000	18.219	18.059
50 000	39.192	38.265
55 000	67.508	64.516
60 000	170.04	150.65

We find that, with exception of the last value, the differences are small in relation to the results obtained by means of the iterative method. The difference in the last value is a consequence of the size of the displacement. This value, however, is no longer accurate, since the entire theory is based on the assumption of small rotations (269), which is no longer acceptable for $P = 60\,000\,N$. An accurate computation, carried out by means of an algorithm

which may be applied irrespective of rotation size [14], yields the results shown in the last column of the following table

P (N)	D_1 (cm) (small rotations)	D_1 (cm) (no rotation limit)
1 000	0.17373	0.17373
2 000	0.35303	0.35303
5 000	0.92709	0.92714
10 000	2.0247	2.0249
20 000	4.9645	4.9652
30 000	9.6289	9.6293
40 000	18.182	18.165
50 000	39.009	38.636
55 000	66.855	64.229
60 000	161.26	123.31
65 000	—	215.35

The second column of this table contains the results yielded by the above described iterative method, considering the exact stiffness for small rotations. In the computation without limiting the size of the rotations, the bars have been considered as axially deformable with a cross-section area of 2000 cm^2 . Figure 182 shows the relations between the load P and the displacement

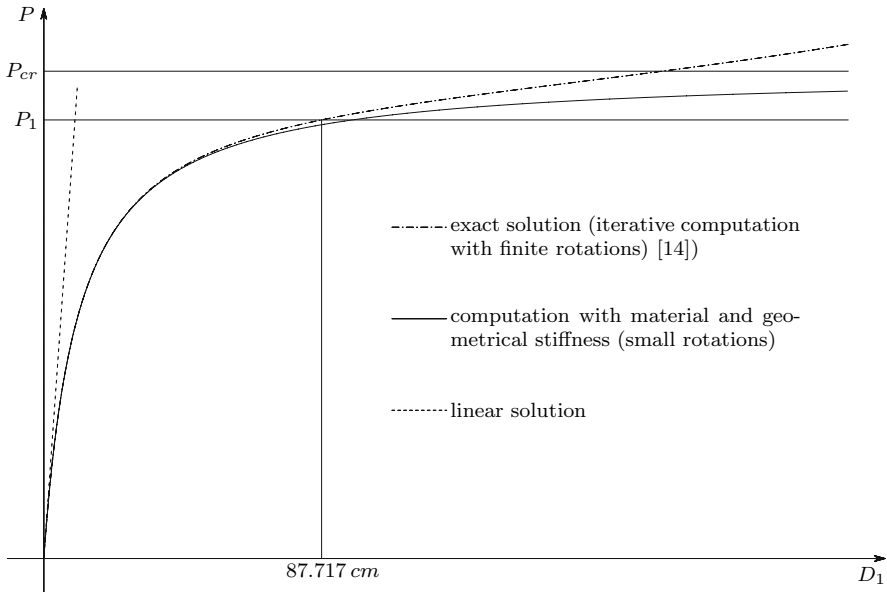


Fig. 182. Relation between P and D_1 in the structure represented in Fig. 181 ($P_1 = 57\,500\text{ N} \approx 0.9 P_{cr}$)

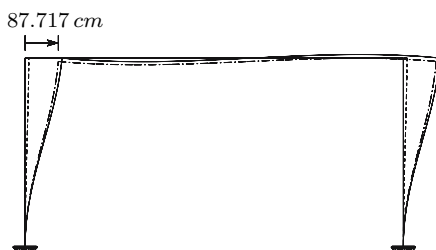


Fig. 183. Deformed configurations of the structure represented in Fig. 181, corresponding to the solution represented in Fig. 182, for $P = 57\,500\text{ N}$

D_1 that have been obtained by the three main types of analysis: linear (only material stiffness); with material and geometrical stiffness and small rotations (the analysis described here), and the analysis without limitation of the size of displacements and rotations [14]. Figure 183 gives the corresponding deformed configurations.

Comparing the results yielded by the methods based on both the exact and the linearized stiffness for small rotations, with the results presented in the third column of the last table, we conclude that all of them give good results until about 90% of the critical load of the structure, (P_{cr} , Fig.182). This is the load that leads to a vanishing determinant of the stiffness matrix, which is obtained assuming small rotations. Actually, this frame supports higher loads without instability, since the tangent stiffness matrix obtained without restriction on the size of the rotations does not become singular, even for substantially higher values of P . This is the reason why it was possible to include the displacement corresponding to $P = 65\,000\text{ N}$ in the last table (215.35 cm).